The Gaseous Environments of Radio Galaxies in the Early Universe: Kinematics of the Lyman α Emission and Spatially Resolved HI Absorption *

R. van Ojik[1], H.J.A. Röttgering[1,2,3], G.K. Miley[1], R.W. Hunstead[4]

[1] *Leiden Observatory, P.O. Box 9513, 2300 RA, Leiden, The Netherlands*

[2] *Mullard Radio Astronomy Observatory, Cavendish Laboratory, Cambridge CB3 0HE, England*

[3] *Institute of Astronomy, Madingley Road, Cambridge CB3 0HA, England*

[4] *School of Physics, University of Sydney, NSW2006, Australia*

* Based on observations collected at the European Southern Observatory, La Silla, Chile, with the WHT on La Palma, Spain and with the AAT, Australia.

R. van Ojik et al.: The gaseous environment of radio galaxies in the early Universe: Kinematics of the Lyman α emission and spatially resolved HI absorption

Main Journal

3. Extragalactic Astronomy

11.01.2, 11.09.1, 11.19.3

H. J. A. Röttgering, Leiden Observatory, Niels Bohrweg 2, P.O. Box 9513, 2300 RA Leiden, The Netherlands, tel. 071-275835

*Based on observations collected at the European Southern Observatory, La Silla, Chile, with the WHT on La Palma, Spain and with the AAT, Australia.

Abstract

We present intermediate resolution ($\sim$ 3 Å) spectra of the Lyα emission from 15 high redshift radio galaxies ($z > 2$). Together with previously published spectra we analyze data for a sample of 18 objects.

In 11 of the 18 radio galaxies we find deep troughs in the Lyα emission profile, which we interpret as H I absorption with column densities in the range 10^{18}–$10^{19.5}$ cm^{-2}. Since in most cases the Lyα emission is absorbed over its entire spatial extent (up to 50 kpc), the absorbers must have a covering fraction close to unity. Under plausible assumptions for the temperature and density of the absorbing gas this implies that the absorbing material must consist of $\sim 10^{12}$ clouds of typical size ~ 0.03 pc with a total mass of $\sim 10^8$ M$_\odot$.

Our observations show that strong H I absorption occurs in $> 60\%$ of the high redshift radio galaxies, while from the statistics of quasar absorption lines there is only a 2% probability of such a strong H I absorption line falling by chance in the small redshift interval of the Lyα emission line. These absorbers are therefore most likely to be physically associated with the galaxy hosting the radio source or its direct environment.

There are strong correlations between the properties of the Lyα emission of the galaxies and the size of the associated radio source: (i) Of the smaller (< 50 kpc) radio galaxies 9 out of 10 have strong associated H I absorption, whereas only 2 of the 8 larger (> 50 kpc) radio galaxies show such strong absorption. (ii) Larger radio sources tend to have larger Lyα emission regions and (iii) a smaller Lyα velocity dispersion than smaller radio sources. The sizes of the Lyα regions range from $\sim$15 to $\sim$130 kpc and radio sizes from $\sim$20 to $\sim$180 kpc. The Lyα velocity dispersions range from $\sim$700 km s^{-1} (FWHM) in the largest radio sources to $\sim$1600 km s^{-1} (FWHM) in the smallest. In the smaller radio sources Lyα is often observed to be more extended than the radio emission.

We have also defined several parameters to describe the spatial distortion of the Lyα velocity field and of the radio structure. We find a strong correlation between the amount of distortion present in the Lyα spectra and the distortion of the radio structure.

These strong correlations show that the radio sources have a profound influence on their environments. The correlations of radio size with the gas velocity dispersion and the Lyα size, are evidence for interaction of the radio jet with the ionized gas.

Three different scenarios to explain these correlations are discussed:

1. The first is based on the properties of the environment. The smaller radio sources are situated in denser (cluster) environments than the larger sources. The relatively dense environment is responsible for the strong extended H I absorptions. Kinetic energy is transferred from the radio plasma to the gaseous medium, resulting in larger line widths and reduced propagation velocities for the radio lobes. The turbulence associated with the radio plasma may expose more gas from dense clouds to the ionizing radiation,

causing the Lyα emission region to have an extent similar to the radio source.

2. The second scenario linking radio size and Lyα is based on evolution of the radio source. When the radio source is small it interacts strongly with the dense central gas, while as it tunnels through the medium to larger sizes the interaction and thus the gas velocity dispersion decreases. The radio size – Lyα size relation has the same origin as in scenario 1.
3. The third scenario is based on orientation effects. If radio galaxies are quasars whose nuclei and broad line regions are obscured towards our line of sight, larger line widths may be expected if we observe closer to the edge of the ionization cone. In this scenario the radio size – Lyα size relation would be simply due to projection effects. The largest radio sources have the largest Lyα sizes with the smallest velocity dispersions because they are oriented closest to the plane of the sky and the broad line regions are most strongly obscured. This would not explain, however, why the largest sources show almost no associated H I absorption.

Key words: Galaxies: active – Galaxies: radio – Galaxies:

1 Introduction

During the last few years we have carried out a programme to enlarge the sample of high-redshift radio galaxies ($z > 2$, HZRGs hereafter), by selecting ultra-steep-spectrum (USS) radio sources (Röttgering 1993; Röttgering et al. 1994). This project has included radio imaging, optical broad-band imaging and spectroscopy. Most of the optical observations were carried out as a Key Programme at the European Southern Observatory in Chile. Until now our USS radio source survey has resulted in the discovery of 29 radio galaxies at redshifts $z > 2$ (Röttgering 1993; Röttgering et al. 1995b; Röttgering et al. 1996; van Ojik et al. 1994; van Ojik et al. 1996), i.e. about half of the total number of galaxies known at such high redshifts. The Lyα emission from HZRGs can be very bright, with fluxes $\sim 10^{-15}$ erg s^{-1} cm^{-2} (luminosities $\sim 10^{44}$ erg s^{-1}), and can extend over more than $10''$ (~ 100 kpc). These Lyα halos are therefore ideal targets for ground-based optical telescopes, providing a powerful tool for studying the gas around the most massive galaxies known in the early Universe.

The morphologies and kinematics of the emission line gas in low-redshift radio galaxies have been studied extensively (e.g. Baum et al. 1992, and references therein). Only now are sufficiently large numbers of HZRGs known to allow such detailed studies at high redshifts so that the properties of the emission line halos at low and high redshifts can be compared. Such a comparison may help to constrain the evolution of the radio galaxies and their environments.

Furthermore, these extended Lyα halos provide an opportunity to observe H I absorption clouds against a spatially resolved background source. Since the late sixties, there have been

extensive studies of absorption lines against the strong continuum emission from quasar nuclei. Because quasars are spatially unresolved, such studies yield no direct information on the spatial scale of the absorbers.† The detection of such absorption clouds against the Lyα emission of HZRGs can, however, provide us with spatial information about the absorbing clouds. An additional advantage of studying absorption against the strong Lyα of HZRGs is that no strong ionizing continuum is (directly) observed from HZRGs that could influence the properties of the absorber.

We have previously presented observations of the Lyα kinematics of two radio galaxies, with strong spatially extended absorption being seen in 0943−242 at $z = 2.9$ (Röttgering et al. 1995a), and complex kinematics in 1243+036 at $z = 3.6$ (van Ojik et al. 1996). Earlier, a high resolution spectrum of the Lyα emission from 4C41.17 has been presented by Chambers et al. (1990). We report here on the results of high spectral resolution observations of a further 15 radio galaxies from our sample.

In Sect. 2 we describe the selection of objects and the observations. In Sect. 3 we present the two-dimensional and one-dimensional Lyα spectra. The spectra are described in detail and parametrized to obtain the properties of the line-emitting gas and H I absorption systems; correlations between the Lyα and radio properties are investigated. In Sect. 4 we discuss the physical properties of the Lyα-emitting gas (including its kinematics and dynamics) and the H I absorption systems, and their relationship with the radio galaxy. We go on to discuss the implications of our work for the dust content of HZRGs and, finally, we put forward three scenarios which may account for the interaction between the radio source and the Lyα emission. We summarize our results and conclusions in Sect. 5.

Throughout this paper we assume a Hubble constant of $H_0 = 50$ km s^{-1} Mpc^{-1} and a deceleration parameter of $q_0 = 0.5$.

2 Source Selection and Observations

The main criterion for the selection of objects from our sample of high redshift radio galaxies was that spectra with good signal-to-noise (S/N) ratio be obtained. We therefore concentrated on the objects with bright Lyα emission and redshifts which placed Lyα in the most sensitive range of the spectrographs and detectors. The S/N ratio at very blue wavelengths is also limited by the transmission of the atmosphere. We therefore selected objects with redshifts $z > 2.1$. As a secondary consideration we gave preference to objects whose spatial extent was large on the low resolution spectra.

High resolution optical spectroscopy was carried out during several different observing sessions. Most of the observations were made with the New Technology Telescope (NTT) of the European Southern Observatory in Chile. One session was with the Anglo-Australian Telescope (AAT) in Australia and one session with the William Herschel Telescope (WHT) on La Palma, Spain (see Table 1). The spectral resolutions ranged from 1.5 to 3 Å FWHM,

†Limited information on the lateral extent of absorbing clouds has come from quasar pairs and gravitationally-lensed quasars with multiple images.

corresponding to 100–200 km s^{-1}, about a factor of ten better than in the low resolution discovery spectra (Röttgering et al. 1996) where the Lyα emission lines are just resolved, with velocity dispersions ∼1000–2000 km s^{-1} (FWHM). A resolution of 2–3 Å is therefore well suited to studying the overall kinematical structure of the emission-line gas and the possible presence of strong H I absorption in the Lyα emission profile.

The ESO NTT observations used the ESO Multi Mode Instrument (EMMI), with the light path split into two arms optimized for observations in the blue and red respectively. Our observations were made in the blue arm where the detector was a Tektronix CCD having 1024×1024 pixels. The scale along the slit was $0.37''$ per pixel; with a slit width of $2.5''$ and ESO grating 3 we achieved a spectral resolution of 2.8 Å. Observations at the WHT were made with the blue arm of the ISIS spectrograph. A 1024×1024 Tektronix CCD was used, giving a scale along the slit of $0.49''$ per pixel. With a slit width of $2''$ and grating R1200B, the spectral resolution was 1.7 Å. At the AAT, the RGO spectrograph was used with a 1024×1024 Tektronix CCD. The spatial scale along the slit was $0.74''$ per pixel, and a $1.6''$ slit and 1200B grating gave a spectral resolution of 1.5 Å (see also Röttgering et al. 1995a). Important parameters for the different observing sessions are summarized in Table 1, where we give the dates of the different sessions, telescopes and instruments, achieved resolutions and an indication of the observing conditions.

The objects were positioned in the slit using blind offsetting from nearby "bright" stars. Due to inaccuracies in the blind offsetting — offsets were sometimes $> 1'$ — the measured line fluxes may be slightly lower than those measured from our low resolution spectroscopy (Röttgering et al. 1996).[‡]

The objects that we observed are listed in Table 2, with the relevant total exposure times, slit position angles and cross-reference to the sessions in Table 1. The spectra were flat-fielded, sky-subtracted and wavelength- and flux-calibrated using the longslit package in the IRAF reduction software of the U.S. National Optical Astronomy Observatory.

3 Results and Analysis

3.1 Description and parameterization of the Lyα spectra

In the following subsections we shall derive various properties and parameters of the Lyα spectra. The two-dimensional spectra are shown in Fig. 1. They have been smoothed slightly with a Gaussian function of $1'' \times 2$ Å FWHM to enhance the most extended Lyα emission. One-dimensional spectra were extracted using apertures which included all extended Lyα emission visible in Fig. 1. These are shown in Fig. 4. Spatial profiles of the Lyα emission, summed over the full spectral range where Lyα emission was detected, are in Fig. 5. The profiles have been smoothed with a Gaussian function of $1''$ FWHM.

[‡]The low resolution spectra were obtained by first taking short images to position the object exactly in the slit.

3.1.1 The Lyα profiles

From the spectra it is immediately clear that many of the radio galaxies have a double- or multi-peaked Lyα velocity profile. The troughs between the peaks have widths of several hundred kilometres per second and in most of them no emission is detected from the bottom of the troughs. However, in several cases the depth of the troughs change with spatial location; a good example of this is 0200+015, where one end of the trough is shallower than the other (see also below).

Because of the steepness of the deepest troughs and the relatively smooth overall velocity profile of Lyα emission, we conclude that the troughs are unlikely to be caused by genuine velocity structure of the Lyα emitting gas but are caused instead by the absorption of Lyα photons by neutral hydrogen very close in redshift. The troughs appear deeper on the one-dimensional spectra of Fig. 4 than on the smoothed two-dimensional ones (Fig. 1), consistent with the absorption features being relatively narrow. The profiles of the deep troughs in the Lyα profiles appear similar to strong absorption lines observed in the spectra of distant QSOs. Most of the QSO absorption lines at such redshifts are interpreted as arising in neutral hydrogen clouds between us and the QSO. It therefore seems likely that the troughs in the Lyα emission profiles of our radio galaxies are also due to H I absorption systems. Although dust mixed through the emission line gas can also effectively absorb Lyα emission due to the large pathlength of the resonant scattering Lyα photons, dust would not be expected to produce such a narrow absorption feature but the entire Lyα emission profile would be depressed and have a more chaotic structure (e.g. 0211−122, see below and van Ojik et al. 1994). We therefore conclude that the deep troughs in the Lyα emission profiles are caused by H I absorption.

In some cases where the S/N is relatively low, we cannot exclude the possibility that the double peaked profile is caused by two separate velocity components of the ionized gas. However, since these profiles are very similar to the profiles with good S/N in which a sharp H I absorption trough is observed, we conclude that the double peak in Lyα profiles observed with lower S/N are also probably due to H I absorption.

We will model the Lyα profile assuming that the underlying Lyα emission line has a Gaussian velocity profile and that the troughs are due to H I absorption characterised by Voigt profiles. We used an iterative scheme that minimized the sum of the squares of the differences between the model and the observed spectrum (see also Röttgering et al. 1995a). Input parameters for this scheme are initial estimates for the redshift, strength and width of the unabsorbed Gaussian emission line and estimates of the redshifts, Doppler parameters and column densities (z, b and N(H I)) of the absorption systems. Most objects show only one obvious absorption feature, but in a few cases there are several (0200+015, 0828+193, 2202+128). The iterative scheme solved for the parameters of the model and we thereby derived the best fit shape of the Gaussian emission line and the redshifts, column densities and Doppler parameters of the H I absorbers.

The modelling of the troughs was not always satisfactory. If an absorption feature appears too complex to be one single absorber, but more likely consists of several absorbers close to each other in redshift, the best fit from the model fitting procedure is not unique and

the derived parameters should be treated with caution. Features in the spectra that are not sharp troughs but are more like "shoulders" in the profile are observed in several objects with the best S/N spectra. These "shoulders" may not be H I absorption but could be due to true velocity structure in the emitting gas. In spite of these possible small deviations from a Gaussian emission profile, the Gaussian approximation appears to be a reasonable description of the overall underlying emission profiles. Modelling these "shoulders" in the Lyα profile with H I absorption requires large Doppler parameters (> 200 km s^{-1}) and relatively low H I column densities (N(H I) $\sim 10^{15}$ cm^{-2}). Large Doppler parameters imply macroscopic motion of the absorbing gas, as a thermal origin would require a gas temperatures of $> 10^5$ K for $b > 50$ km s^{-1} and $> 10^6$ K for $b > 200$ km s^{-1} (see also Section 4). To ensure that the iterative scheme did not diverge for those objects with a "shoulder" in the Lyα profile and a strong narrow (N(H I) $> 10^{17}$ cm^{-2}) absorption feature, such broad "shoulders" were also modelled by H I absorption. In the section on individual objects we illustrate these difficulties for a few cases.

The one-dimensional Lyα profiles and the adopted model-fits of the objects are displayed in Fig. 4. The derived parameters (z, b and N(H I)) of the absorption systems are listed in Table 3. In this table $z_{Ly\alpha}$ is the redshift of the peak of the original emission line profile (assumed Gaussian) that was modelled with the iterative fitting of emission and absorptions. The absorbers for each object are numbered in order of the H I column density, z_1 being the redshift of the strongest H I absorption system in an object. The redshifts of the emission and absorbers were determined after converting the wavelengths to vacuum values and have an estimated accuracy of ~ 0.0002. The resultant width of the original (unabsorbed) Lyα emission line is listed in Table 4, which lists all determined parameters of the Lyα emission.

3.1.2 Extent and mass of the Lyα gas

From the two-dimensional spectra the spatial extent of the Lyα emission regions varies from 2″–17″ between the sources. We can define a total extent by simply measuring the maximum extent to which Lyα emission is seen at $> 2\sigma$ level in Fig. 1. We denote this extent by $D^{tot}_{Ly\alpha}$. However, this measure is not a good indicator of the scale size of the Lyα extent because the spectra have different integration times and sensitivities. Furthermore, the flux level of the most extended Lyα emission may depend on the central Lyα flux of an object and thus could be below the detection limit of our spectra for the objects with low Lyα luminosity. To obtain a more robust measure of the Lyα extent, we have extracted spatial profiles of the Lyα by summing the columns over the wavelength range where Lyα was detected in Fig. 1. From these spatial profiles we define a scale size of the Lyα emission, $D^{20\%}_{Ly\alpha}$, as the extent between the spatial points where the Lyα emission flux is 20% of the peak level. This 20% level is chosen because it can still be measured reliably in the spectra with the lowest S/N ratio in our sample. Both $D^{20\%}_{Ly\alpha}$ and $D^{tot}_{Ly\alpha}$ are listed in Table 4.

We can estimate the mass of the Lyα emitting gas from the integrated Lyα luminosity as measured from our spectra. After obtaining the density of the ionized gas assuming case B recombination through $L = 4 \times 10^{-24} n_e^2 f_v V$ erg s^{-1} (McCarthy et al. 1990), where V is the total volume occupied by the emission line gas and f_v the volume filling factor of the gas, the

mass in ionized gas is M$\approx n_e m_{proton} f_v V$ (McCarthy et al. 1990). The volume filling factor of the ionized gas must be estimated because we have no means of determining it directly for our HZRGs. From direct measurements, using sulphur lines, of the density of line emitting gas in low redshift radio galaxies, filling factors in the range 10^{-4}–10^{-6} and typically of order $\sim 10^{-5}$ have been deduced (van Breugel et al. 1985b; Heckman et al. 1982). We will assume this value for the Lyα emission line regions of our HZRGs. For a more detailed discussion of the ionization of the Lyα emission line region in HZRGs see e.g. McCarthy et al. (1990), Chambers et al. (1990), McCarthy (1993), van Ojik et al. (1996). Calculating the volume of the measured Lyα emission from the defined $D^{20\%}_{Ly\alpha}$ and the width of the slit and taking the depth of the Lyα region the same as the transverse size (i.e. the slit width) we find that the masses of Lyα emitting gas in the radio galaxies of our sample are are typically a few times 10^8 $M_\odot$ (see Table 4).

3.1.3 Spatial structure in the Lyα spectra

When examining the two-dimensional spectra it is apparent that in many cases the spatial position of the maximum intensity of the Lyα emission varies as a function of wavelength. In some cases the peak position changes smoothly with wavelength (e.g. 0748+134) while in others it varies in a more irregular manner (e.g. 0828+193, 2202+128). We have measured this spatial position of the maximum Lyα intensity per wavelength bin ($S_M(\lambda)$), where the extent of a wavelength bin varied from 2–4 pixels to obtain a reasonable S/N per bin so that the position could be determined with an accuracy of no worse than a few tenths of an arcsecond. Note that these measurements of the spatial position of the maximum intensity of Lyα at different wavelengths ($S_M(\lambda)$) is not the same as used to measure velocity structure in spectra, where at every spatial position the wavelength of the maximum intensity of the emission line profile is determined (thus $\lambda_M(S)$). For the objects with brightest Lyα the position variations were measured on the unsmoothed frames, while the fainter were measured from the smoothed frames of Fig. 1. The errors on the positions depend on the S/N level of the Lyα emission in each wavelength bin. The regions of the spectra where a strong H I absorption is present were excluded. The galaxy 1707+105 was excluded from these measurements because it has at least two spatial maximums at the position of two galaxies situated along the radio axis. We also give positional changes from the two-dimensional Lyα spectrum of radio galaxy 1243+036 (van Ojik et al. 1996). The results are shown in Fig. 6.

From Fig. 6 we see that indeed most objects show significant changes in the spatial positions as a function of wavelength (or velocity). The amplitude of these changes vary from a few tenths of an arcsecond to several arcseconds. In some spectra the spatial position changes gradually while some others have several spatial "wiggles". We will parameterize the positional changes in two ways. The first is the amplitude, $\Delta S = S_M^{max} - S_M^{min}$, which is simply the distance between the most extreme spatial positions of maximum Lyα intensity measured (S_M^{max} and S_M^{min}), whose accuracy is still better than $\sim 0.5''$. This amplitude does not indicate whether there is a smooth gradient or if there are several discrete "wiggles". Therefore, we introduce another parameter that indicates the amount of "wiggles" in the positional changes relative to the velocity range over which the positions are measured.

This "wiggling index", $w_S = n_S/\Delta v$, is (an estimate of) the number of different positional gradients along the velocity profile, n_S (or the number of times that the positional gradient changes, plus one), divided by the velocity range (Δv, in thousands km s^{-1}) of the interval measured.

In Table 4 we list all measured Lyα properties. In this table we have also included the additional objects 1243+036 (van Ojik et al. 1996), 0943-242 (Röttgering et al. 1995a) and 4C 41.17 (Chambers et al. 1990) from which similar high resolution spectra have been published. In some cases we found that the Lyα fluxes at high resolution were smaller than those measured in the low resolution spectra (Röttgering et al. 1996; van Ojik et al. 1994; van Ojik et al. 1996) from which the redshifts were determined. Various factors can contribute to this discrepancy, e.g. differing seeing or photometric conditions, or small errors in the telescopes blind offsetting for the high resolution spectroscopy. Therefore the objects for which we have determined the Lyα fluxes only from the high resolution spectroscopy are marked in Table 4. Due to the large sizes of the Lyα emission regions, it is likely that the limited width of the slit (2.5″) of the spectrograph did not cover the entire transverse extent of the Lyα emission (see e.g. 1243+036). We estimate that the true Lyα fluxes of the galaxies may well be a factor 2 higher than those determined from our high resolution spectroscopy. The columns give the following parameters:
(1) the source name
(2) the velocity width (FWHM) of the Gaussian fitted to the Lyα emission profile (section 3.1.1)
(3) indication whether strong H I absorption ($> 10^{17}$ cm^{-2}) is present: 1: yes; 0: no
(4) 20% projected linear size of the Lyα emission region (20% of the peak level in Fig. 5)
(5) total observed projected linear size of the Lyα region ($> 2\sigma$ in Fig. 1)
(6) logarithm of the Lyα luminosity
(7) mass of the Lyα emitting gas
(8) the total H I mass derived from the column density and size of the absorber (Section 4)
(9) the distance between the most extreme spatial positions of maximum Lyα intensity in the spectrum
(10) The number of different positional gradients of the maximum Lyα intensity along the velocity profile as seen in Fig. 6
(11) The "wiggling index", $w_S = n_S/\Delta v$, the number of positional gradients of Lyα (column 10) divided by the velocity interval over which the Lyα positions were measured

3.2 Remarks on individual objects

In this section we discuss in detail the Lyα spectra of several of the most interesting objects from the sample. This will illustrate that in at least some of these systems there is clear observational evidence that dust, broad emission lines or accompanying galaxies play an important role. It will also illustrate some of the limitations of the fitting procedure that we applied to obtain parameters of the absorption systems. For the full list off remarks on objects we refer to an Electronic Appendix.

0211−122: This radio galaxy has a peculiar optical spectrum in which the Lyα emission

is anomalously weak compared to the higher ionization lines. This anomaly has been interpreted as being produced by dust mixed through the emission line gas which partly absorbs the Lyα emission (van Ojik et al. 1994). The two-dimensional high resolution spectrum of the Lyα shows a clearly different structure than the rest of the galaxies in our sample. There is one small region with strong Lyα emission that is relatively narrow (300 km s^{-1} FWHM) and is responsible for more than one third of the flux. Furthermore, there are several weaker patches of Lyα emission distributed around the bright peak. The bright narrow peak is spatially offset by $\sim 1''$ from the peak of the continuum emission. This somewhat peculiar two-dimensional Lyα profile is consistent with the interpretation of van Ojik et al. (1994) that dust is mixed through the Lyα emitting gas of 0211−122. The bright narrow peak may be a region where the dust content is sufficiently low so that the Lyα photons can escape. In spite of the different appearance of the velocity field, the integrated line profile does show a double peaked shape. Although this double peaked appearance may be produced by dust within the Lyα region, it is also possible that an H I absorption system plays a role.

If we model the observed profile as being due to H I absorption of an originally Gaussian profile, we obtain a fit as displayed in Fig. 2 with a very narrow ($\sim$700 km s^{-1} FWHM) Lyα having a strong H I absorption of column density N(H I)=$10^{19.5}$ cm^{-2}. However, the centre of this absorption is not as opaque as it should be with such a strong absorption (see also the two-dimensional spectrum in Fig. 1). There is more Lyα emission from the bottom of the trough than in any of the other galaxies with strong HI absorption. Thus it seems unlikely that this simple model is correct. An alternative fit is given by a less luminous original emission profile, thus ignoring most of the emission from the bright narrow peak and giving an HI column density of $\sim 10^{18}$ cm^{-2} (displayed in Fig. 4). However, this fit is also not well matched to the observed profile. It may be that the profile is purely due to dust mixed with the ionized gas, extinguishing the resonant scattering Lyα photons, although we cannot exclude that H I absorptions contribute to the shape of the Lyα profile of 0211−122.

0828+193: The Lyα profile has a spectacular shape. The emission is very strong but drops steeply on the blue side of the peak, while slightly further bluewards some Lyα emission is visible again. Thus, it appears that almost the entire blue wing of the Lyα emission profile has been absorbed. Also the most extended and fainter emission shows the same sudden drop at 4343 Å. This is a remarkable radio galaxy that has a close ($\sim 3''$) companion along its radio axis (Röttgering et al. 1995b). The presence of a close companion, from which no Lyα emission is detected, suggests that a neutral gaseous halo of this galaxy might be responsible for the absorption of the blue wing of the Lyα emission from 0828+193. However, it is not certain that the companion is at the same redshift, because no emission lines are detected. Also in the red wing of the Lyα profile, a broad shoulder is observed that may be due to multiple H I absorption systems or may be caused by intrinsic velocity structure of the Lyα emitting gas.

The steepness of the absorption trough next to the Lyα peak requires the absorber to have an H I column density of $\sim 10^{18.3}$ cm^{-2}. But the broadness of the absorption, extinguishing nearly all emission in the blue wing of Lyα, requires the Doppler parameter for a single absorber to be ~ 162 km s^{-1}. This fit is displayed in Fig. 2. This absorption fit has removed too much of the original Lyα profile, as there is clearly emission observed just blueward of

the sharp drop to zero at $\sim$ 4340 Å. Thus, the absorption may be due to the combination of several absorption systems at slightly different velocities with respect to the Lyα peak. The few small emission peaks that are left of the Lyα blue wing, are significant and can be well modelled by assuming three distinct absorbers (see Fig. 4). The main absorber has a column density of $\sim 10^{18.1}$ cm^{-2} and the other two are $\sim 10^{16.3}$ cm^{-2} with more reasonable Doppler parameters of 16 to 80 km s^{-1}. Although the absorption may be even more complex, this model is the simplest one that gives a satisfactory fit so we adopted these values. The broad shoulder in the red wing is also modelled by HI absorption with a large gas velocity dispersion, but we cannot exclude that it is caused by true velocity structure in the Lyα emitting gas.

1357+007: This galaxy which is associated with a small (3″) radio source has a deep trough in the Lyα profile. The Lyα profile has a relatively low S/N. The one-dimensional spectrum of this object is a good example for demonstrating the difference between modelling the troughs as being due to H I absorption and as being due to true velocity structure. The limitations of the models are illustrated by comparing the best fits obtained by a two velocity component emission model (Fig. 3) with those from an absorption model (Fig. 4). The fit of the Lyα emission profile by a combination of two Gaussian emission profiles at different velocities is less satisfactory than the H I absorption model. This is because the trough between the two peaks on the profile is steeper than the wings on the outside of the emission peaks. Although we cannot exclude the possibility of a non-Gaussian but symmetric double peaked emission profile, this difference in steepness of the trough and the outer wings of the emission profile is accounted for by a Voigt absorption profile which is also the best fit for the troughs in the profiles with the best S/N. The actual situation may be more complicated than implied by the idealized assumptions of the models, but it seems that also in 1357+007 H I absorption is the more plausible interpretation in spite of the lower S/N ratio than in our best spectra.

1436+157: This is a quasar–galaxy pair oriented along the radio axis (like the galaxy-galaxy pair 0828+193). There is no direct evidence that the galaxy is at the same redshift as the quasar; only the quasar shows strong Lyα emission. Apart from very broad Lyα emission and strong continuum, as is common for quasars, the Lyα has a spatially extended narrow component. This is why we include it in our sample. A strong H I absorption feature is present in the narrow line component over the entire Lyα extent. The extended Lyα emission is larger than the radio source. Part of the emission may be due to the companion galaxy or a tidal interaction if the companion galaxy is indeed associated with the quasar.

The strong H I absorption feature in the narrow line Lyα component requires a very large Doppler parameter of $\sim$200 km s^{-1} when modelled by one single absorber. Although we cannot exclude the possibility of an absorber with such a large intrinsic velocity dispersion, a better fit to the data is obtained by a model of two or more absorbers. In Fig. 3 the fit is shown that we obtain for two adjacent absorbers, each with an H I column density of about $10^{19.3}$ cm^{-2} and Doppler parameters of 12–75 km s^{-1}. We have also extracted a spectrum of the off-nuclear Lyα emission by only summing the spectra beyond a distance of 2″ from the peak of the continuum (shown in Fig. 4). Although there is still some contamination from the quasar continuum in this spectrum, the contribution of broad Lyα emission is negligible. To fit the off-nuclear profile, either a single absorber with large Doppler parameter ($\sim$250

km s^{-2}) is needed or more than one absorber. As a most plausible fit we have adopted a two absorbers model, whose parameters are in Table 3.

3.3 Correlations between the physical parameters

The data presented here for the first time allow the properties of the Lyα to be compared with other properties of high redshift radio galaxies to search for statistical correlations. In Table 5 we list some of the main radio properties of the objects from Röttgering et al. (1994), Carilli et al. (1996) and Chambers et al. (1990).

The radio galaxies for which high resolution radio maps are available (Carilli et al. 1995) show large variation in the complexity of the radio morphologies, from a simple straight double structure with or without a nucleus to bent morphologies with double hot spots. To indicate the amount of distortion of the radio morphology we define a "distortion index", ξ_{radio}, as the number of lines with significantly different position angles that connect the different components in a radio source. This index not only indicates the presence of bending on the scale of the total extent of the radio source but also takes into account the presence "wiggles" caused by multiple hot spots. Although ξ_{radio} is somewhat subjective, dependent on the size of a radio source and the resolution on the radio maps, it does indicate the relative differences in distortion between the radio sources. The columns of Table 5 contain the following:
(1) the source name
(2) largest projected angular size of the radio emission from 1.5 GHz VLA maps, which are available for all sources. The sizes measured at 8 GHz (for the sources that were also observed at this frequency) do not differ significantly from those at 1.5 GHz.
(3) transverse radio size; projected size perpendicular to the main radio axis (from 2), measured from 1.5 or 8 GHz maps
(4) the radio "distortion index", ξ_{radio}
(5) radio spectral index between 178 or 365 or 408 MHz and 2.7 or 5 GHz (see Röttgering et al. 1994)
(6) radio core fraction (ratio of core flux to total radio flux) at a rest frequency of 20 GHz
(7) ratio Q of the distances between the radio core at 4.7 GHz, or optical identification (superposed on the 4.7 GHz maps or 1.5 GHz) and the brightest feature in each radio lobe
(8) ratio of the integrated flux densities of the radio lobes (maximum/minimum)
(9) logarithm of the monochromatic radio power at a rest frequency 1.5 GHz, estimated from the flux at 1.5 GHz and the spectral index.

For more details on the definitions of the radio properties see Carilli et al. 1996; Röttgering et al. 1994 and McCarthy et al. 1991.

3.3.1 Lyα size and velocity dispersion

We have investigated if there are correlations between the various parameters as listed in Tables 4 and 5. A strong correlation were found between the radio size and Lyα size, $D^{20\%}_{Ly\alpha}$, and a strong anti-correlation between the radio size and the velocity width (FWHM) of the

Lyα emission. These two correlations are shown in Fig. 7. We chose to show only the correlation with $D^{20\%}_{Ly\alpha}$ as this is the most objective measure of the scale of Lyα extent of the sources, although the total observed Lyα size ($D^{tot}_{Ly\alpha}$) also correlates strongly. A Spearman rank correlation analysis shows that the anti-correlation of radio size with the Lyα velocity width has significance level of 99.8% and the correlation between the Lyα size and the radio size has a significance higher than 99.9%.

There is also a somewhat weaker anti-correlation between the Lyα size and the Lyα velocity width (see Fig. 8), that has a significance of 99.6% in a Spearman rank correlation analysis. A partial correlation analysis of the Lyα size and the Lyα velocity width, controlling for the radio size, gives a low significance of only 71.4% for this anti-correlation, an order of magnitude worse than for the two strong correlations when controlling for the third property. This suggests that the apparent anti-correlation between the Lyα size and the Lyα velocity width just reflects the first two correlations. Thus, we conclude that the size and velocity dispersion of the Lyα emitting gas in our sample of high redshift radio galaxies has a strong dependence on the size of the associated radio source. The smaller radio sources have smaller Lyα emission regions but with a higher Lyα velocity dispersion.

We further note that in 11 of the 18 of the objects the total measured Lyα extent ($D^{tot}_{Ly\alpha}$) is larger than the radio source.

3.3.2 HI absorption

Strong H I absorption (N(H I)$> 10^{18}$ cm^{-2}) mainly occurs in the objects with the smaller associated radio sources and Lyα emission region (see Fig. 7). In 9 out of the 10 radio galaxies smaller than 50 kpc strong H I absorption is found, while only in 2 out of 8 with radio sources larger than 50 kpc. Note that the latter include the peculiar galaxy 0211−122 where the absorption of Lyα may not be entirely due to H I.

The Lyα luminosity of the objects and the Lyα velocity width show no significant correlation (Fig. 8). A notable feature from this plot is that the average Lyα luminosity of the radio galaxies with strong associated H I absorption is about a factor 2 lower than those without a strong associated H I absorber. Although this suggests that the H I systems might be responsible for absorbing $\sim 50\%$ of the Lyα flux, the large dispersion in the luminosities (the errors on the mean luminosities of both samples are more than a factor of 2), this difference is not statistically significant.

In Fig. 9 we show a histogram of the relative velocity of the strong absorption systems with respect to the peak of the original (Gaussian) Lyα emission profile as obtained from the modelling. The median velocity is at a blueshift of ~ 100 km s^{-1}. It is noteworthy that in almost all cases the strong H I absorption is within ~ 250 km s^{-1} of the Lyα peak. Only in one case (0828+193) the absorption is at a substantially larger velocity of ~ 540 km s^{-1}. We have tested whether this might be a selection effect, in that we would not be able to distinguish the absorption systems if they had larger relative velocities. After restoring the original Lyα emission spectra for those objects with strong H I absorption, by filling in the absorption troughs using the absorption line profiles obtained from the Lyα profile fitting,

and simulated the similar absorptions at larger relative velocities. We find that we would have clearly distinguished the H I absorption systems in the Lyα profiles out to velocities of almost half the FWHM of the Lyα emission, i.e. 450–700 km s^{-1}. In the spectra with the highest S/N, absorption systems would have been distinguished out to velocities even further than half the FWHM. Thus we conclude that the velocity distribution with 90% of the absorption systems within $\sim$ 250 km s^{-1}, is real.

3.3.3 Lyα position shifts

We have found that the spatial position of the maximum intensity of the Lyα emission changes as a function of wavelength and sometimes shows several "wiggles" over the wavelength range of the emission line (Fig. 6). Neither the maximum amplitude of the position shifts, ΔS, nor the "wiggling index", w_S, correlate with any of the other Lyα parameters, such as size and velocity dispersion. But, although ΔS does not show an apparent correlation with the largest linear size (i.e. measured along the radio axis) of the radio source, there is a (weak) correlation (96.5% from a Spearman rank analysis) with the transverse size (projected size perpendicular to the radio axis) of the radio source (Fig. 10). It appears that the radio sources with larger transverse sizes tend to have larger Lyα shifts. Note that sources for which there is only an upper limit of the transverse radio size have relatively small Lyα position shifts. This implies that the actual relation would probably be stronger if the true transverse sizes of these sources were known.

A strong correlation ($> 99.9\%$) exists between the distortion index of the radio (ξ_{radio}), and the Lyα "wiggling index" (w_S) (see Fig. 10). Thus, the sources with the most distorted radio morphologies also show the most "wiggles" in the Lyα peak position.

Distortion of radio sources, i.e. bending and multiple hot spots, increases the transverse size of a radio source, producing the correlation between ΔS and the transverse radio size.

4 Discussion

4.1 The Lyα emission

4.1.1 Physical properties

From previous low resolution studies it is known that HZRGs usually have extended (up to 100 kpc), luminous ($\sim 10^{44}$ erg s^{-1}) Lyα halos with velocity dispersions of > 1000 km s^{-1} FWHM (see McCarthy 1993 and references therein). Our high spectral resolution study confirms these general properties. The total detected spatial extent of the Lyα halos ranges from $\sim$ 15 kpc to 135 kpc, while the velocity dispersions range from 700 km s^{-1} to 1600 km s^{-1} (FWHM).

The detected Lyα emission often extends further than the radio lobes. In the cases where this very extended emission is detected with good S/N, it appears to have a lower velocity

dispersion than the inner Lyα halo. This is most clearly seen in the objects 1243+036 (van Ojik et al. 1996), 0200+015, 0828+193 and 4C41.17 (Chambers et al. 1990). In these cases the Lyα emission can be divided into two components: an "inner halo" which has dimensions smaller than the radio source and which has a large velocity dispersion (700–1600 km s^{-1} FWHM), and an "outer halo", outside the radio structure, which is relatively quiescent ($\sim$ 300 km s^{-1} FWHM). This relatively quiescent outer halo combined with more violent kinematics inside the radio structure is most clearly apparent in the spectacular radio galaxy 1243+036 at $z = 3.6$ (van Ojik et al. 1996).

McCarthy et al. (1991) found that the extended emission line gas of 3C radio galaxies (median redshift 0.4) is generally asymmetric and brightest on the side of the radio lobe closest to galaxy nucleus, which also tends to be the brightest radio lobe (46 out of 70). In our sample of high redshift ($z > 2$) radio galaxies, 7 of the 17 galaxies have clearly asymmetric Lyα emission regions, i.e. the surface brightness of the extended Lyα emission is larger on one side of the galaxy than on the other. Only 3 of these 7 have the brightest extended Lyα emission on the side of the closest radio lobe and thus do not show the correlation with lobe arm length asymmetry that McCarthy et al. (1991) found for the 3C galaxies (37 out of 39). However, 6 of these 7 have the brightest extended Lyα emission on the side of the brightest radio lobe, while McCarthy et al. found this correlation only weakly present in his 3C sample. We note that the statistics of our sample are poor with only 7 measured asymmetric emission line regions against 39 galaxies of McCarthy et al. (1991). One of the reasons why we do not find the same asymmetry correlation may be because the extended emission line regions of HZRGs are usually much larger and smoother, sometimes larger than the radio sources, than those of the intermediate redshift 3C sample of McCarthy et al. (1991), who also noted this difficulty in measuring the asymmetry of Lyα in HZRGs. Another possibility is that the inconsistency is due to the fact that we measure the Lyα emission, while McCarthy et al. (1991) measured the extent of [OII]λ3727. Different mechanisms may determine the spatial distribution of Lyα and [OII] emitting gas.

It has been suggested that the emission line gas in radio galaxies may be responsible for the depolarization of the radio emission (e.g. van Breugel et al. 1985a and 1985b and references therein). The depolarization of the radio emission is also often observed to be asymmetric (Carilli et al. 1995). A strong anti-correlation between asymmetric depolarization of the radio emission from quasars with the side of the quasar on which the radio jet is observed (Garrington et al. 1988; Laing 1988) and large rotation measures of the polarized radio emission in HZRGs (Carilli et al. 1994; Carilli et al. 1995) have been interpreted as evidence that a hot (10^7 K) magnetoionic halo surrounding the objects causes the depolarization and that the asymmetry is caused by the orientation of the radio source in the hot halo. If the depolarization of the radio emission is caused by the emission line gas or an associated hotter gas component, one would expect that asymmetry of the extended emission line regions would correspond to asymmetric depolarization of the radio emission. For most of the galaxies in our sample high resolution radio polarization measurements have been carried out by Carilli et al. (1996). Most of the radio galaxies have asymmetric polarization, where one radio lobe is much more depolarized than the other. Polarization information is available for only 5 of the 7 sources with asymmetric Lyα emission in our sample. In only 2 of these 5, the fractional polarization is lowest on the side of the most extended Lyα

emission, indicating that line asymmetry – polarization asymmetry at least does not have a strong correlation. However, this result is statistically too poor to indicate whether the Lyα emitting gas plays an important role in the depolarization of radio emission in our sample of HZRGs or not.

4.1.2 Ionization of the Lyα emission line region

Several authors have argued that the large equivalent width of the Lyα emission as well as the line ratios of the emission lines associated with radio galaxies in general are not well reproduced by shock ionization nor by hot stars and that anisotropic photoionization by an obscured nucleus appears to be the dominant mechanism of ionization (Baum & Heckman 1989a; Baum & Heckman 1989b; Baum et al. 1992; McCarthy 1993; Ferland & Osterbrock 1986; Ferland & Osterbrock 1987; McCarthy 1993; Charlot & Fall 1993; Antonucci & Miller 1985; Antonucci 1993; McCarthy et al. 1990; Chambers et al. 1990; McCarthy 1993; van Ojik et al. 1996). In our sample of HZRGs we have found a strong relation between the radio size and Lyα size, which suggests that the radio plasma interacts with the ambient gas. Shock ionization associated with the impact of the radio jet and with the expansion of the radio lobes might explain this direct size relation. However, the spatial emission profiles show that Lyα emission is strongest near the center of the galaxies and decreases rapidly with distance in the halo, instead of being brightest at the extremities where the radio lobe has just passed. Furthermore, the presence of Lyα emission from the region outside the radio structure in more than half our objects cannot be produced by shocks associated with the radio sources, but argues strongly for photoionization of the emission line gas by a central continuum source. The relation between the sizes of Lyα and the radio source must be produced by a different mechanism (see Section 4.3). We conclude that the Lyα emission line region is most likely produced by (anisotropic) photoionization by a central continuum source.

4.1.3 Kinematics and dynamics

The velocity dispersion of the Lyα emitting gas in our sample of HZRGs varies from $\sim$700–1600 km s^{-1}. Such large velocity dispersions were already known from low resolution studies (see McCarthy 1993 and references therein) and are similar to the velocity dispersion of extended Lyα emission seen in some radio-loud quasars (Heckman et al. 1991a). Interaction between the radio source with the emission line gas has been suggested as a cause for high velocity dispersions in radio galaxies the (de Young 1981; van Breugel et al. 1985b; de Young 1986; McCarthy et al. 1990; Chambers et al. 1990). In the high redshift quasars, Heckman et al. (1991) were unable to establish a definite connection between the velocities of the extended emission line gas in quasars and the radio source. They note that such large velocity dispersions may also have a gravitational origin if gas is falling in from large radii in the process of galaxy formation (see also Fall & Rees 1985).

Apart from the velocity dispersions we have observed detailed velocity structure in the Lyα emission line region. We have found that in several of the individual objects the velocity

profile shows small deviations from a Gaussian profile ("shoulders" on the wings of the profiles) and occasionally there are signs of rotation. Furthermore, the spatial position of the maximum intensity of Lyα often varies with wavelength ("wiggles"). These features in the velocity structure indicate that the Lyα emission line region is not one system with purely chaotic gas motions, but also contains some large scale motions.

We have found several strong correlations between the velocity structure of the Lyα emitting gas and the properties of the radio source:
(i) an anti-correlation between the size of the radio source and the velocity dispersion of the Lyα emitting gas. The smaller radio sources have larger Lyα velocity dispersion.
(iii) The number of "wiggles" in the Lyα position with wavelength correlates with the amount of distortion of the radio structure.
(ii) the component of the Lyα emitting gas that is extended beyond the radio source has a lower velocity dispersion than the gas inside the radio structure.

As noted by Heckman et al. (1991) and Fall & Rees (1985), the high velocity dispersions typically found in HZRGs can be gravitational in origin. If the radio galaxies are at the bottom of a deep potential well, i.e. a dense cluster, gas falling in from large radii can reach velocities of more than 1000 km s^{-1}. Individual infalling gas regions, ionized by the active nucleus as they come near the center of the radio galaxy, could also produce spatial "wiggles" in the Lyα velocity structure. However, such a gravitational origin of the Lyα velocity structure does not produce any of the observed correlations with the radio source properties. Furthermore, the relatively constant velocity dispersion inside the radio structure and the sudden decrease outside the radio source, is inconsistent with a gravitational infall scenario.

The three correlations indicate that the kinematics of the Lyα are connected with the radio source. We have earlier presented convincing evidence that the radio source accelerates and disturbs the emission line gas in the radio galaxy 1243+036 (van Ojik et al. 1996). In this galaxy the radio jet is bent at the position of an "accelerated" region of emission line gas. Further, 1243+036 has a quiescent (250 km s^{-1} FWHM) outer Lyα halo, while inside the radio source the Lyα emitting gas has a large velocity dispersion (1575 km s^{-1} FWHM). Our current observations have provided two more objects (0200+015, 0828+193) where the velocity dispersion of the Lyα emitting gas outside is lower than inside the radio structure. Similar quiescent Lyα gas is also present outside the radio structure in 4C41.17 (Chambers et al. 1990). We conclude that the interaction of the radio plasma with the gas in our HZRGs is responsible for the large velocity dispersions inside the radio structure and the spatial "wiggles" in the Lyα velocity structure.

On the basis of spectroscopy of low redshift radio galaxies, Baum et al. (1992) classified these radio galaxies in three kinematical classes: (i) rotators, associated with recent mergers, (ii) calm non-rotators that are identified with cooling flows and (iii) violent non-rotators, that have optical and radio morphologies similar to the rotators, but whose kinematics are dominated by large chaotic gas motions overshadowing any signs of rotation. Because of the similarities in their optical and radio properties, Baum et al. (1992) suggested that the rotators and violent non-rotators may be kinematically linked, but that original rotation in the violent non-rotators has been "washed out" by the interaction with the powerful radio

source. The HZRGs that we have investigated here show relatively large velocity dispersions (> 1000 km s^{-1} FWHM) of the ionized gas when compared to the low redshift radio galaxies that have velocity dispersions a few hundred km s^{-1} (FWHM) of Baum et al. (1992). Only in a few cases (0748+134, 1410−001 and 1558−003) there is a hint of a velocity shear over the extent of the Lyα emission region, that could be attributed to a relic of rotation beneath the large turbulent velocities of the ionized gas. In 1243+036 (van Ojik et al. 1996) we found "calm" rotational kinematics of the Lyα gas outside the radio structure, while inside the radio plasma the ionized gas has a large (1500 km s^{-1} FWHM) velocity dispersion and the kinematics are dominated by chaotic motions. In the rest of our sample of HZRGs there is often Lyα emission extended beyond the radio structure with apparently a lower velocity dispersion, but these outer halos do not show signs of rotation, except in 0200+015. In this galaxy the Lyα emitting gas extending beyond the radio source appears to have a velocity shear at least on one side of the galaxy where the H I absorption also remains present over the same extent. Using the criteria of Baum et al. (1992) none of these galaxies would classify as rotators, because the kinematics are dominated by large turbulent motions and evidence for rotation is only weakly present in a few cases. The interpretation of 1243+036 (van Ojik et al. 1996) that turbulence induced by the propagating radio source "washes out" the signs of rotation, and the few hints of rotation in several galaxies with lower than average gas velocity dispersions, supports the idea of Baum et al. (1992) for the low redshift radio galaxies, that the rotators and violent non-rotators are linked. Hence, all our powerful high redshift radio galaxies may well have originally had rotating gas halos, due to a galaxy interaction or from the accretion of gas from the primeval environment. However, any clear rotation signature has been washed out by large turbulent motions due to interaction with the propagating radio plasma.

4.2 HI absorption systems

4.2.1 Physical properties and kinematics

Our observations show that high redshift radio galaxies often have very strong and extended H I absorption systems seen against their Lyα emission. Evidence of such absorption was given by the observations of Hippelein & Meisenheimer (1993), who imaged the Lyα emission of 4C41.17 using a Fabry–Pérot system. They found a relatively weak H I absorption, of $\sim 10^{15}$ cm^{-2} column density, with a projected size of $\sim 10 \times 10$ kpc^2, covering a part of the Lyα emission region of 4C41.17 at $z = 3.8$. They interpret this absorption as due to a fortuitously intervening Lyα forest absorption.

A small hint of this absorption is visible in the high resolution spectrum of Chambers et al. (1990). The strong absorptions that we find in our sample of radio galaxies appear to be different from the weak absorption in 4C41.17 in that they are more than 3 orders of magnitude stronger and up to 5 times more spatially extended. Our observations show that in the cases where strong absorption (N(H I) $> 10^{18}$ cm^{-2}) is seen against the Lyα emission of the radio galaxy, the absorber extends over the entire size of the emission line region with observed projected sizes up to ~ 50 kpc. However, the strength of the absorption is not always the same over all spatial scales. The largest Lyα emitting regions with H I absorption

show more Lyα emission from the bottom of the absorption trough (e.g. 0200+015) than the objects with small Lyα emission regions (e.g. 2202+128). The depth of the absorptions over such different scales indicates that the covering factor of absorbing material must be close to unity over scales of ∼20 kpc, and still of the order of 0.9 on ∼50 kpc scales.

From the sizes and derived column densities of the absorbers and assuming that the size of the absorbers along the line of sight is the same as the observed transverse size, we find that the mass in neutral hydrogen of an absorption system is M(H I)=10^8 $R_{35}^2 N_{19}$ $M_\odot$, where R_{35} = 35 kpc is the average size the absorption systems in our sample and N_{19} = 10^{19} cm^{-2} the characteristic H I column density. The H I masses deduced for the individual objects is listed in Table 4 and range from ∼ 10^7–10^8 $M_\odot$. The total hydrogen mass of the absorption systems depends on the ionization state of the gas. Photoionization models of absorption systems with column densities in the range of those observed in our radio galaxies (N(H I)= 10^{18}–10^{20} cm^{-2}) by Bergeron (1988) and Bergeron & Stasińska (1986), indicate that the ratio of H II/H I averaged over the whole absorption cloud is in the range 4–250. Although the conditions in the extended absorption systems in our HZRGs may be different from those in the line of sight to quasars, they are shielded from the direct ionizing radiation from the radio galaxy. The range of ionization parameters found for the gas in H I absorption systems by Bergeron & Stasińska (1986) that are assumed to be ionized by the intergalactic UV radiation field, is the same as that estimated in the narrow emission line regions of quasars and radio galaxies (see McCarthy 1993), although the ionization source is different. Therefore, the H II/H I ratio in the absorption systems in our HZRGs may not be very different from the absorption systems modelled by Bergeron (1988) and Bergeron & Stasińska (1986). Thus, the total mass in hydrogen in the observed absorption systems is probably in the range of 0.4–250 x 10^8 $M_\odot$. This total mass in the absorption systems covering the extent of the Lyα emission is similar to the masses we estimated for the Lyα emitting gas itself in these HZRGs.

Assuming that the clouds of the absorption systems are confined by external pressure, we can try to derive some properties of these clouds (see also Röttgering et al. 1995a). There is strong evidence from X-ray observations and depolarization measurements that radio galaxies at low and high redshifts are surrounded by hot (∼ 10^7 K) gas (e.g. Arnaud et al. 1984; Henry and Henriksen 1986; Crawford and Fabian 1993; Carilli et al. 1994). From the balance of the minimum pressures of the radio plasma of HZRGs and the external hot gas, we find a typical external pressure nT ∼ 10^6 cm^{-3} K (e.g. Chambers et al. 1990; McCarthy 1993; Carilli et al. 1994; van Ojik et al. 1996). As mentioned above, absorption systems of H I column densities 10^{18}–10^{20} cm^{-2} are predominantly ionized, and their temperatures are maximally a few times 10^4 K (Bergeron 1988; Bergeron & Stasińska 1986). Observations of quasar absorption systems with low column densities (10^{12}–10^{14} cm^{-2}) indicate that temperatures in those absorption systems may be lower than ∼5000–10 000 K (Pettini et al. 1990).

Because the various observations appear to indicate temperatures around 10^4 K, we shall assume a temperature of 10^4 K for the absorption systems in our HZRGs as a working assumption in the following. For pressure balance between the absorbing gas and the external medium (nT ∼ 10^6 cm^{-3} K), the gas density would then be ∼ 100 cm^{-3}. The mass, density and size of the absorption systems indicate that the gas only occupies a small fraction of the

volume of the absorption system. The volume filling factor is given by $f_v = N/Rn$, where N is the HI column density, R is the size of the absorption system (assuming the depth of the system is the same as the observed size along the slit) and n is the density of the gas. The volume filling factor for the extended absorption systems in our sample of radio galaxies then range from a few times 10^{-7} to a few time 10^{-6}. With an average size of an absorption system of $R_{35} = 35$ kpc, gas density $n_{100} = 100$ cm^{-3} and H I column density $N_{19} = 10^{19}$ cm^{-2}, the volume filling factor of the absorption systems is:

$$f_v \sim 10^{-6} N_{19} R_{35}^{-1} n_{100}^{-1}$$

However, the absorption systems may contain more ionized than neutral hydrogen, which would imply a higher volume filling factor. From the typical mass in H I of the absorption systems, $M_8 = 10^8$ M$_\odot$, and the ratio of total hydrogen mass to H I mass defined as $r =$ M(H)/M(H I) the volume filling factor is:

$$f_v \sim 10^{-6} r M_8 R_{35}^{-3} n_{100}^{-1}$$

Although this is only a crude estimate of the filling factor, depending very much on the external pressure, the temperature of the absorbing gas and on the assumed geometry of the absorption systems, we adopt the value of $f_v = 10^{-6}$ to estimate the sizes of the individual clouds. The size of an individual cloud is estimated by $d = Rf_v/f_c$. This size can be derived since we know the covering fraction of the clouds in the absorption system f_c to be close to unity. For a typical absorption system size of 35 kpc, the individual clouds have sizes of ~ 0.035 pc. To cover the projected surface of the absorption system, it must contain $\sim 10^{12}$ such clouds (corresponding to $\sim$4x10^8 M$_\odot$, consistent with an H II/H I ratio of a few). If the individual clouds are not spherical but filamentary, as may be likely, the number of such clouds would change, but the derived size would be the average size of individual clouds along the line of sight.

The large Doppler parameters that are often required for an optimum fit to the absorption profiles are too large to be only due to thermal motions of the gas, because they would imply gas temperatures of $\sim 10^6$ K. The width of the absorption lines may be due to a superposition of a large number of absorbing clouds covering the velocity range or be due to macroscopic gas motions in the absorbing clouds. We can estimate the velocity dispersion of the gas from the Doppler parameter and the temperature of the gas, where $b = (2kT/m + 2\sigma^2)^{1/2}$ where m is the mass of hydrogen and σ is the gas velocity dispersion (see Cowie and Songaila 1986). Assuming a maximum temperature of the absorbing gas of 10^4 K, for Doppler parameters 50–200 km s^{-1} the gas velocity dispersion σ is 35–140 km s^{-1}.

4.2.2 Relation to the radio galaxy and Lyα emission

From the statistics of quasar absorption lines, the chance of a random intervening absorber with column density larger than 10^{18} cm^{-2} in the small redshift interval of the Lyα emission line ($\Delta z \sim 0.03$) is only $\sim$2–3% (e.g. Petitjean et al. 1993). Our sample of high redshift radio

galaxies has a high incidence of ∼60% of such strong associated absorption, and even ∼90% of the radio sources with radio size smaller than 50 kpc. Thus these absorption systems are much more common than in quasars and cannot be random intervening absorbers, but must be intrinsic to the radio galaxies or their direct environment.

One possibility might be that a strong absorption is caused by the gaseous halo of a neighbouring galaxy if the radio sources reside in clusters. There is evidence from some damped Lyα absorption systems (Briggs et al. 1989) and from the statistics of Lyα absorption in the line of sight of gravitationally lensed QSOs that high redshift galaxies may have halos of more than 10 kiloparsec (e.g. Smette et al. 1992 and references therein). Assuming that cluster galaxies have a hydrogen halo size of 35 kpc (the average size of the observed extent of the H I absorbers and consistent with the size estimates derived from the statistics of Lyα absorptions in QSOs) and a typical cluster size of 1 Mpc, this would imply $\sim$ 200 such galaxies to cover all lines of sights to the radio galaxy. Such a density of galaxies with large hydrogen halos in a cluster around the radio source seems unlikely. Furthermore, the typical velocity dispersion in low and intermediate redshift clusters is $\sim$ 1000 km s^{-1}. However, the H I absorption systems in our HZRGs are almost always within 250 km s^{-1} of the peak of the Lyα emission profile (see Section 3.3, Fig. 9).

Alternatively, the absorption may be caused by a large tidal remnant of an interaction with a companion galaxy (Röttgering et al 1996b). However, it is implausible that, even if all our radio galaxies have had an interaction, such tidal remnants would in 60–90% of the cases be exactly located in our line of sight to the Lyα emission and covering its entire extent. Furthermore, if quasars are in similar cluster environments as radio galaxies, one would expect a similar high incidence of associated absorptions in quasars if they are caused by cluster galaxies or tidal remnants, which is not observed.

In orientation-based unification models radio galaxies and radio loud quasars are regarded as intrinsically similar objects, viewed from different angles (see Antonucci 1993; Barthel 1989 and references therein). Due to an obscuring torus of dust and gas surrounding the active nucleus, the radiation from the nucleus can only be observed within a cone which is oriented along the radio axis. This anisotropic radiation ionizes the gas clouds in its path resulting in an extended emission line region. In quasars the radio/cone axis is oriented close to the line of sight and we therefore observe the bright ionizing continuum and broad-line emission region close to the nucleus, while in radio galaxies the nucleus is obscured so that we cannot observe the ionizing radiation directly.

In this scenario, both quasars and radio galaxies must have a large envelope of gas surrounding the entire systems. In radio galaxies the ionizing cone is close to the plane of the sky and we see the emission line region from the side. Our line of sight to the Lyα emission region would pass through the region of gas outside the cone of ionizing radiation (see Fig. 11). This gas is not affected by the propagating radio plasma, that is presumed to have stirred up the emission line gas, causing high velocity dispersions. This much more quiescent gas outside the ionizing cone is the most likely cause of the strong absorption in the Lyα emission line profiles. If indeed both the Lyα emitting gas and the absorbing gas are components of the extended gaseous envelope of the galaxy, it would also explain why in all observed cases the absorption systems extend over the entire Lyα emission region.

Suggestive evidence for this interpretation is also that the estimated masses for the amount of emission line gas are roughly similar to the estimated total masses (neutral and ionized gas) of the absorption systems (typically a few times 10^8 $M_\odot$). The presence of H I outside the ionization cone has been directly observed in the low redshift ($z = 0.022$) Seyfert 2 galaxy NGC 5252 (Almudena Prieto & Freudling 1993).

We note that although this interpretation may work as a general picture for the HZRGs, there are several individual cases where the situation must be more complicated (e.g. 1243+036, 0828+193, 1436+157). The presence and strength of H I absorption in an individual case may also depend on e.g. the total amount of gas present in a radio galaxy, the power of the nuclear ionizing continuum, differences in cone opening angle and the presence of an extra (isotropic) ionization source (starburst) and interaction with companion galaxies.

If the gas of the absorption systems is indeed from the same gaseous envelope as the Lyα emitting gas, the high covering factor (0.9–1) of the absorbing gas does not imply that the gas located within the ionization cone has the same high covering factor in clouds that are *optically thick* to the nuclear ionizing continuum radiation. If the degree of ionization increases by a factor of 10 inside the ionization cone, the covering fraction of optically thick clouds would decrease to $\sim$ 0.1, the value that is estimated for extended Lyα emission observed in high redshift radio loud quasars (Heckman et al. 1991b). Note that this same mechanism probably causes the "inverse" or "proximity" effect in quasars, where there is a strong decrease of the number of Lyα absorption systems close to the redshift of the quasars (e.g. Murdoch et al. 1986; Lu et al. 1991).

It is interesting that, although there does not seem to be a large excess of associated absorption in QSOs in general, there is a tendency for associated absorption to occur preferentially in steep spectrum radio loud quasars (Foltz et al. 1988; Anderson et al. 1987; Barthel et al. 1990; Heckman et al. 1991a). The incidence rate of associated absorptions in radio loud quasars is about 16% within 2000 km s^{-1} of the quasar redshift. Radio loud quasars also have more extended line emission than radio quiet QSOs (Heckman et al. 1991b). These properties suggest that both radio loud galaxies and radio loud quasars at high redshifts reside in denser environments than radio quiet and flat spectrum objects. Furthermore, their larger relative velocities and lower occurrence rate compared to the associated absorption in our sample of HZRGs suggests that they may not have the same origin and are more consistent with being due to neighbouring cluster galaxies rather than being intrinsic to the quasars themselves.

We note that the associated absorption systems in these radio galaxies are quite different from the broad (several thousands km s^{-1}) absorption line systems that are observed in some quasars.

4.2.3 Implications for the dust content of HZRGs

A comparison of optical with infrared measurements show that high redshift radio galaxies have a Lyα/Hα ratio lower than was expected for case B recombination by a factor of 2–10 (McCarthy et al. 1992; Eales et al. 1993; McCarthy 1993). This has been interpreted as

being most likely due to dust mixed with the emission line gas, selectively destroying the resonant scattering Lyα photons. Other evidence for the presence of dust comes from optical polarization measurements, that indicate that much of the extended continuum light may be scattered continuum radiation from an obscured AGN (Tadhunter et al. 1992; Cimatti et al. 1993; Cimatti et al. 1994; di Serego Alighieri et al. 1994).

Our observations of the Lyα profiles have shown that neutral hydrogen is present in many HZRGs and can absorb $\sim$50% of the original Lyα emission. Thus, the low observed Lyα/Hα ratios are at least in part due to associated H I absorption systems (see also Röttgering et al. 1995a).

We note that to effectively destroy Lyα emission by dust, the dust must be distributed homogeneously through the ionized gas. Because of the low volume filling factor of the emission line gas, a Lyα emission region with low dust content or non-homogeneous dust distribution will produce strong Lyα emission from the galaxy. The radio galaxy 0211−122 appears to be an exceptional case where the dust distribution meets this stringent geometrical requirement well enough to effectively extinguish most of the Lyα emission (see van Ojik et al. 1994)). While very little dust distributed homogeneously can extinguish all Lyα emission, for different geometries galaxies could contain large amounts of dust without destroying the Lyα emission. Differences between the distribution of dust and Lyα emitting gas are not unlikely because dust is probably produced by star formation in the galaxy itself and transported outwards into the gaseous halo while the Lyα halo gas may well originate from accretion from the primeval environment.

The geometrical requirement of H I absorption of Lyα is much less stringent than for absorption by dust. The H I clouds must be non-uniformly distributed around the emission line gas and located in our line of sight to reduce the observed Lyα emission flux. Only if neutral gas clouds were exactly uniformly distributed around the radio galaxies, the observed flux in our line of sight would not be reduced, in spite of the random scattering of the Lyα photons in the H I clouds.

Thus, because of the presence of associated H I absorption in HZRGs, which reduces the observed Lyα flux, the dust content of HZRGs derived from the Hα/Lyα ratio may have been overestimated. In the near future, more accurate polarization measurements with 8-metre class telescopes and continuum measurements with new mm-wavelength instrumentation and the ISO satellite along with spectroscopy of more IR emission lines, will be crucial to determine the true dust content of these primeval galaxies.

4.3 The Lyα – radio source connection: scenarios

Perhaps the most remarkable results from our study relate the Lyα emission and absorption to the radio properties of high redshift radio galaxies. Firstly, the small radio sources almost always have strong associated H I absorption. The large radio sources show very little associated H I absorptions and have narrower Lyα velocity widths. Secondly, there is a strong anti-correlation between the radio size and velocity width of Lyα. Thirdly, there is a strong correlation between the radio size and the size of the Lyα emission region. The bigger radio

sources have larger Lyα emission regions associated with them. Fourthly, variations in the spatial position of the maximum intensity of Lyα as a function of wavelength ("wiggles") correlate with the amount of distortion of the radio morphology.

These relations between the Lyα and radio properties are strong evidence for a kinematic interaction between the radio jet and the ambient gas. In the case of 1243+036 there is direct and convincing morphological evidence for vigorous interaction between the radio source and the Lyα gas (van Ojik et al. 1996). We note that a similar relation between radio power and [OIII] width was noted by Heckman et al. (1981) for low redshift radio sources and Seyfert galaxies and was taken as evidence for a radio–gas interaction.

As we have argued in Section 4.1, shock-ionization associated with the expansion of the radio lobes is probably not the cause of the Lyα size – radio size correlation, because there are several indications that the Lyα is mainly ionized by a central continuum source. The radio plasma may have another effect on the ambient gas, namely to increase the amount of Lyα emission from the region inside the radio lobes by the mechanism suggested by Bremer et al. (1996): Because the luminosity depends on the volume filling factor of the gas, interaction of the radio jet and turbulence in the radio lobes may rip apart neutral cores of emission line clouds therefore increasing the filling factor, exposing more gas to the ionizing continuum and increasing the Lyα emission. Outside the radio structure, gas (with lower filling factor) can also be photoionized but Lyα emission is at a lower flux level. This mechanism has the advantage that it can explain the radio size – Lyα size relation, without the inconsistencies of a shock-ionization interpretation (see Section 4.1).

The "wiggles" in the Lyα position as a function of wavelength indicate that there are large regions of gas having velocities different from the mean velocity at different positions with respect to the centre of the galaxy. The "wiggles" in the Lyα position usually occur on scales of less than an arcsecond, while the distortions of the radio structure tend to be large scale phenomena. In several objects the radio source has double hot spots at its extremities, at $\sim$ 20 kpc from the nucleus while the Lyα "wiggles" are within 5 kpc of the centre of the galaxy. This indicates that, although the Lyα "wiggles" correlate with the degree of distortion of the radio sources, they do not necessarily coincide spatially. Possibly, interaction of the radio jet with the ionized gas near the centre of the galaxy at an earlier epoch has resulted in the current radio distortions on larger scales, while the current Lyα–radio interaction induces a future bent morphology and multiple hot spots of the radio source.

Scenarios

Apart from the possible nature of the "wiggles" in the Lyα position as a function of wavelength and the relation between Lyα size and radio size which were discussed above, we need to explain the correlations of the radio size with the velocity dispersion of the Lyα emitting gas and the presence of associated H I absorption. We propose three different scenarios, one environmental, one evolutionary and one based on orientation:

1. *Environmental scenario* The environment of a massive galaxy in which a radio source resides, will influence the size evolution and morphology of the radio source and the observed Lyα properties. In a dense (proto-cluster) environment a radio source will vigorously interact with the ambient gaseous medium. Kinetic energy will be transferred from the radio source to the gas, increasing the velocity dispersion of the gas and reducing the propagation speed of the radio source. Therefore the radio source stays relatively small. The Lyα emission from the gas that is ionized by photoionization and possibly shocks shows strong H I absorptions from the dense gas in the direct environment. In a low density environment, the propagating radio source will encounter much less resistance and reach to a large size. There will be relatively little interaction with the environment, a smaller velocity dispersion and no clouds large and dense enough to produce strong H I absorption of the Lyα emission.

This would be consistent with the work of Baum et al. (1989) who at low redshifts finds that the smaller powerful 3C sources are generally more depolarized, have more complex emission line morphologies and more distorted radio structures. Fifty percent of these objects are known to be at the centers of rich (cooling flow) clusters. The larger 3C radio galaxies have more normal polarization and less distortion. These galaxies are isolated or reside in small groups of galaxies, where there may be less material to interact with. Thus the coincidence of larger Lyα velocity dispersion and H I absorption with the smaller and sometimes more distorted radio structures in our $z > 2$ sample, may be evidence that these galaxies are at the centers of dense (proto-)clusters. The larger radio sources have simpler Lyα kinematics and no strong absorptions and they are probably more isolated galaxies or reside in less dense clusters.

In a denser environment one might expect the Lyα luminosity to be higher because this scales strongly with the density of the emission line gas (the Lyα luminosity scales as $L \sim n_e^2 f_v V$ erg s^{-1}, where n_e is the density of the gas, f_v the volume filling factor and V the volume occupied by the emission line gas, see McCarthy et al. 1990). We do not find any evidence for such a correlation in our observations. However, not only the gas density but also the total volume of an emission line region determines the Lyα luminosity. While the environment of the larger radio sources has a lower density, the sizes and therefore the volume occupied by the Lyα emission line region is much larger than for the smaller sources. Therefore the total Lyα luminosity of the larger sources may not be very different from the smaller sources. Furthermore, the presence of strong H I absorption also reduces the observed Lyα luminosity of the smaller sources. Finally, also the large variation of the Lyα luminosities (by a factor of 30 between the individual objects) makes it difficult to any possible evidence of a correlation between the density of the environment and the Lyα luminosity.

2. *Evolutionary scenario* In this scenario the small radio sources are at different stages in their evolution than the larger radio sources. As the radio source propagate outwards it first encounters a dense gaseous medium whose velocity dispersion is increased via transfer of kinetic energy from the radio jet and we observe a small radio source with Lyα emission of relatively large velocity width. The dense parts of the gaseous medium that have not (yet) been affected by the interaction with the radio source would produce strong absorption in the Lyα emission. As the radio source propagates further outwards there is less interaction

as the ambient density decreases with radius and the radio jet has cleared a path through the denser inner parts of the galaxy's halo. The velocity dispersion of the gas then reduces due to dissipation and less direct interaction with the radio source.

The main problem of this evolutionary scenario is to explain the decrease of extended HI absorption clouds as the radio source propagates outwards. In the case of shock ionization the clouds may become ionized as the boundary of the radio lobe passes through the neutral gas. However, as described above, shock ionization is unlikely to be dominant enough to ionize the H I absorption systems. Furthermore, the possible disruption of the neutral clouds by the passage of the radio lobes will not prevent them from producing H I absorption features, because the gas will still be shielded from the central ionizing continuum.

3. *Orientation scenario* A third way of producing the observed correlation between the projected radio and Lyα size and the anti-correlation with the velocity dispersion of the gas might be in the context of the orientation-based unification schemes of quasars and radio galaxies (as explained earlier). Close to the active nucleus the velocity dispersion of the gas is high (many thousands of kilometres per second), while further out the gas velocities decrease. Smaller radio sources have their radio axes oriented preferentially closer to our line of sight. In that case we would also see a smaller emission line region and, as we observe closer into the nuclear region, we may see more gas with a larger velocity dispersion. This scenario however does not explain why smaller radio sources (oriented towards our direction) are more likely to have extended H I absorption than larger ones (those closer to the plane of the sky). We should then also observe associated H I absorption in quasars as frequently as in radio galaxies, which is not the case. In fact the opposite would be more likely in an orientation scenario, if the absorbing gas is outside the cone of ionizing radiation from the AGN.

West (1993) has argued that the radio axis of radio galaxies and quasars may actually be oriented along the direction of mass distribution in (proto) clusters and that the formation of clusters and their brightest galaxy would occur through infall along this direction. If this is the case there would be more mass present along the direction of the radio axis so for objects whose axes are oriented closer to our line of sight there would be more (neutral) gas in the absorbing path. However, as mentioned earlier, the velocity dispersion in a cluster is of the order of 1000 km s^{-1} while the strong H I absorptions are much narrower and almost always within $\sim$ 250 km s^{-1} of the Lyα emission peak (Fig. 9).

A possible indication of the angle between the radio axis and our line of sight would be the radio core fraction (e.g. Browne & Perley 1986; Browne & Murphy 1987). For radio sources oriented closer to our line of sight it is expected that the radio flux from the core is a larger fraction of the total radio flux than for radio sources oriented closer to the plane of the sky. We see no evidence for a such relation between the Lyα velocity dispersion and the radio core fraction (Tables 4 and 5; see also Carilli et al. 1996). This suggests that orientation effects do not play an important role in the observed correlations.

Because of the problems that the evolutionary and orientation scenario have with explaining the presence of strong H I absorption preferentially in the smaller radio sources, we favour the environmental explanation for the observed velocity–size correlation. Additional

evidence for the importance of environmental effects comes from observations of 1243+036 at $z = 3.6$ where the morphological correspondence between the radio and the Lyα emission indicates that there is clear vigorous interaction between the radio source and the surrounding gas (van Ojik et al. 1996). Thus we find that it is likely that many steep spectrum HZRGs reside in a dense environment, possibly a (proto) cluster.

5 Conclusions

Our high resolution spectroscopic study of Lyα emission in high redshift radio galaxies has shown the following:
1) The Lyα velocity profiles show considerable detailed structure much of which is indicative of H I absorption.
2) Strong H I absorption with column densities 10^{18}–$10^{19.5}$ is found against the Lyα emission in 11 of 18 objects. Almost all our galaxies (9 out of 10) with (projected) radio sizes smaller than 50 kpc, have strong H I absorption. For the galaxies with larger radio sources, there is only occasional evidence for associated H I absorption
3) The H I absorbers are spatially extended over the entire Lyα emission region, indicating that they have a covering fraction near unity over a region of $\sim$50 kpc.
4) The overall Lyα kinematics are dominated by turbulent motions. Only in a few cases there is a hint of large scale organized dynamics, possibly rotation. On smaller scales the Lyα spectra there is also evidence that the kinematics are not purely chaotic, such as "shoulders"in the velocity profile and "wiggles" in the spatial position of the maximum intensity of Lyα as a function of velocity.
5) The Lyα emission is usually sharply peaked near the centre of the radio galaxy and the Lyα emission often extends beyond the size of the radio source. The detected extent of the Lyα emission regions range from 15 to 135 kiloparsec.
6) There is a strong correlations between the radio size and the Lyα size and a strong anti-correlation between the radio size and the velocity dispersion of the emission line gas. The smaller radio sources have larger gas velocity dispersions and smaller emission line gas regions than the larger radio sources.
7) The amount of "wiggling" of the Lyα position as a function of velocity correlates strongly with the amount of distortion of the radio source morphology and the amplitude of the wiggling correlates with the transverse radio size.

These observations have the following implications:
a) The frequent occurrence of strong H I absorption systems is much too large to be caused by random intervening absorbers. The absorbers must be directly associated with the radio galaxy or its environment.
b) On the basis of orientation-unification scenarios of radio galaxies and quasars, the H I absorption systems may well be due to gas from the gaseous halo of the galaxy, situated outside the ionization cone. Halos of neighbouring cluster galaxies or tidal tails from galaxy interactions seem very unlikely causes for the H I absorptions.
c) The large velocity dispersions of the ionized gas and the wiggles in the Lyα peak spatial position as a function of velocity are best explained as due to interaction of the radio plasma

with the gas.
d) The correlation between Lyα properties and radio properties and the frequent presence of associated H I absorption indicate that HZRGs are located in dense environments. The smaller radio sources most likely reside in the densest (cluster) environments, where large amounts of neutral gas are present and most interaction with the radio source occurs. Transfer of kinetic energy from the radio jet to the gas increases the gas velocity dispersion and reduces the propagation speed of the radio source.

There is considerable scope for following up on these observations. First, it is important to make similar measurements in a range of position angles and not just confined to the radio position angle. Secondly, more detailed imaging of the Lyα halos will help delineate the geometry of the individual Lyα halos. Thirdly, HST imaging and spectroscopic observations will allow the details of the gas and its kinematics to be studied in the important nuclear regions. Fourthly, small high redshift radio sources with large gas velocity dispersions and strong associated H I absorptions are excellent targets in searching for clusters of galaxies in the early Universe.

One intriguing question that remains is what role the gas clouds play in galaxy evolution. The typical sizes of 40 lightdays deduced for individual clouds are comparable with that of the solar system. It is tempting to speculate that these clouds are intimately associated with the early formation stages of individual stars and that they delineate a fundamental phase in galaxy evolution.

Acknowledgements

We would like to thank Malcom Bremer useful discussions. We acknowledge support from an EU twinning project, funding from the high-z programme subsidy granted by the Netherlands Organization for Scientific Research (NWO) and a NATO research grant. RWH acknowledges financial assistance for this programme from the Australian Research Council.

References

Almudena Prieto M., Freudling W., 1993, ApJ 418, 668
Anderson S. F., Weyman R. J., Foltz C. B., Chaffee F. H., 1987, AJ 94, 278
Antonucci R., 1993, ARA&A 31, 473
Antonucci R., Miller J., 1985, ApJ 297, 621
Arnaud K. A., Fabian A. C., Eales S. A., Jones C., Forman W., 1984, MNRAS 211, 981
Barthel P. D., 1989, ApJ 336, 606
Barthel P. D., Tytler D. R., Thomson B., 1990, A&AS 82, 339
Baum S. A., Heckman T. M., 1989a, ApJ 336, 681
Baum S. A., Heckman T. M., 1989b, ApJ 336, 702
Baum S. A., Heckman T. M., van Breugel W., 1992, ApJ 389, 208
Bergeron J., 1988, In: Blades J. C., Turnshek D., Norman C. A. (eds.) QSO Absorption Lines: Probing The Universe. Cambridge: University Press, p. 127
Bergeron J., Stasińska G., 1986, A&A 169, 1
Bremer M. N., Fabian A. C., Crawford C. S., 1996, in press
Briggs F. H., Wolfe A. M., Liszt H. S., Davis M., Turner K. L., 1989, ApJ 341, 650
Browne I. W. A., Murphy D. W., 1987, MNRAS 226, 601
Browne I. W. A., Perley R. A., 1986, MNRAS 222, 149
Carilli C. L., Owen F. N., Harris D. E., 1994, AJ 107, 480
Carilli C. L., Röttgering H. J. A., van Ojik R., et al., 1996, in press
Chambers K. C., Miley G. K., van Breugel W. J. M., 1990, ApJ 363, 21
Charlot S., Fall S. M., 1993, ApJ 415, 580
Cimatti A., di Serego Alighieri S., Field G. B., Fosbury R. A. E., 1994, ApJ 422, 562
Cimatti A., di Serego Alighieri S., Fosbury R. A. E., Salvati M., Taylor D., 1993, MNRAS 264, 421
Cowie C. C., Songaila, A., 1986, ARA&A 24, 499
Crawford C., Fabian A., 1993, MNRAS 260, L15
de Young D. S., 1981, Nat 293, 43
de Young D. S., 1986, ApJ 307, 62
di Serego Alighieri S., Cimatti A., Fosbury R. A. E., 1994, ApJ 431, 123
Eales S. A., Rawlings S., Puxley P., Rocca-Volmerange B., Kuntz K., 1993, Nat 363, 140
Fall S. M., Rees M., 1985, ApJ 298, 18
Ferland G., Osterbrock D., 1986, ApJ 300, 658
Ferland G., Osterbrock D., 1987, ApJ 318, 145
Foltz C., Chaffee F., Weymann R., Anderson S., 1988, In: Blades J. C., Turnshek D., Norman C. (eds.) QSO Absorption lines: Probing the Universe. Cambridge: Cambridge University Press, p. 53
Garrington S. T., Leahy J. P., Conway R. G., Laing R. A., 1988, Nat 331, 147
Heckman T. M., Lehnert M. D., Miley G. K., van Breugel W., 1991a, ApJ 381, 373
Heckman T. M., Lehnert M. D., van Breugel W., Miley G. K., 1991b, ApJ 370, 78
Heckman T. M., Miley G. K., van Breugel W. J. M., Butcher H. R., 1981, ApJ 247, 403
Heckman T. M., van Breugel W. J. M., Balick B., Butcher H. R., 1982, ApJ 262, 529
Henry J. P., Henriksen M. J., 1986, ApJ 301, 689
Hippelein H., Meisenheimer K., 1993, Nat 362, 224

Laing R. A., 1988, Nat 331, 149
Lu L., Wolfe A. M., Turnshek D. A., 1991, ApJ 367, 19
McCarthy P., Spinrad H., van Breugel W., et al., 1990, ApJ 365, 487
McCarthy P. J., 1993, ARA&A 31, 639
McCarthy P. J., Elston R., Eisenhardt P., 1992, ApJ 387, L29
McCarthy P. J., van Breugel W., Kapahi V. K., 1991, ApJ 371, 478
Murdoch H. S., Hunstead R. W., Pettini M., Blades J. C., 1986, ApJ 309, 19
Petitjean P., Webb J. K., Rauch M., Carswell R. F., Lanzetta K., 1993, MNRAS 262, 499
Pettini M., Hunstead R. W., Smith L. J., Mar D. P., 1990, MNRAS 246, 545
Röttgering H. J. A., 1993, Ph.D. thesis, University of Leiden
Röttgering H. J. A., Lacy M., Miley G. K., Chambers K. C., Saunders R., 1994, A&AS 108, 79
Röttgering H. J. A., Hunstead R., Miley G. K., van Ojik R., Wieringa M. H., 1995a, MNRAS 277, 389
Röttgering H. J. A., Miley G. K., Chambers K. C., 1995b, A&AS 114, 51
Röttgering H. J. A., van Ojik R., Miley G. K., et al., 1996a, A&A, in press
Röttgering H. J. A., West M. J., Miley G. K., Chambers K. C., 1996b, A&A, 307 376
Smette A., Surdej J., Shaver P. A., et al., 1992, ApJ 389, 39
Tadhunter C. N., Scarrott S., Draper P., Rolph C., 1992, MNRAS 256, 53p
van Breugel W., Filippenko A. V., Heckman T. M., Miley G., 1985a, ApJ 293, 83
van Breugel W. J. M., Miley G. K., Heckman T. M., Butcher H., Bridle A., 1985b, ApJ 290, 496
van Ojik R., Röttgering H. J. A., Carilli C., et al., 1996, A&A, in press
van Ojik R., Röttgering H. J. A., Miley G. K., et al., 1994, A&A 289, 54
West M., 1994, MNRAS 268, 79

6 Figures

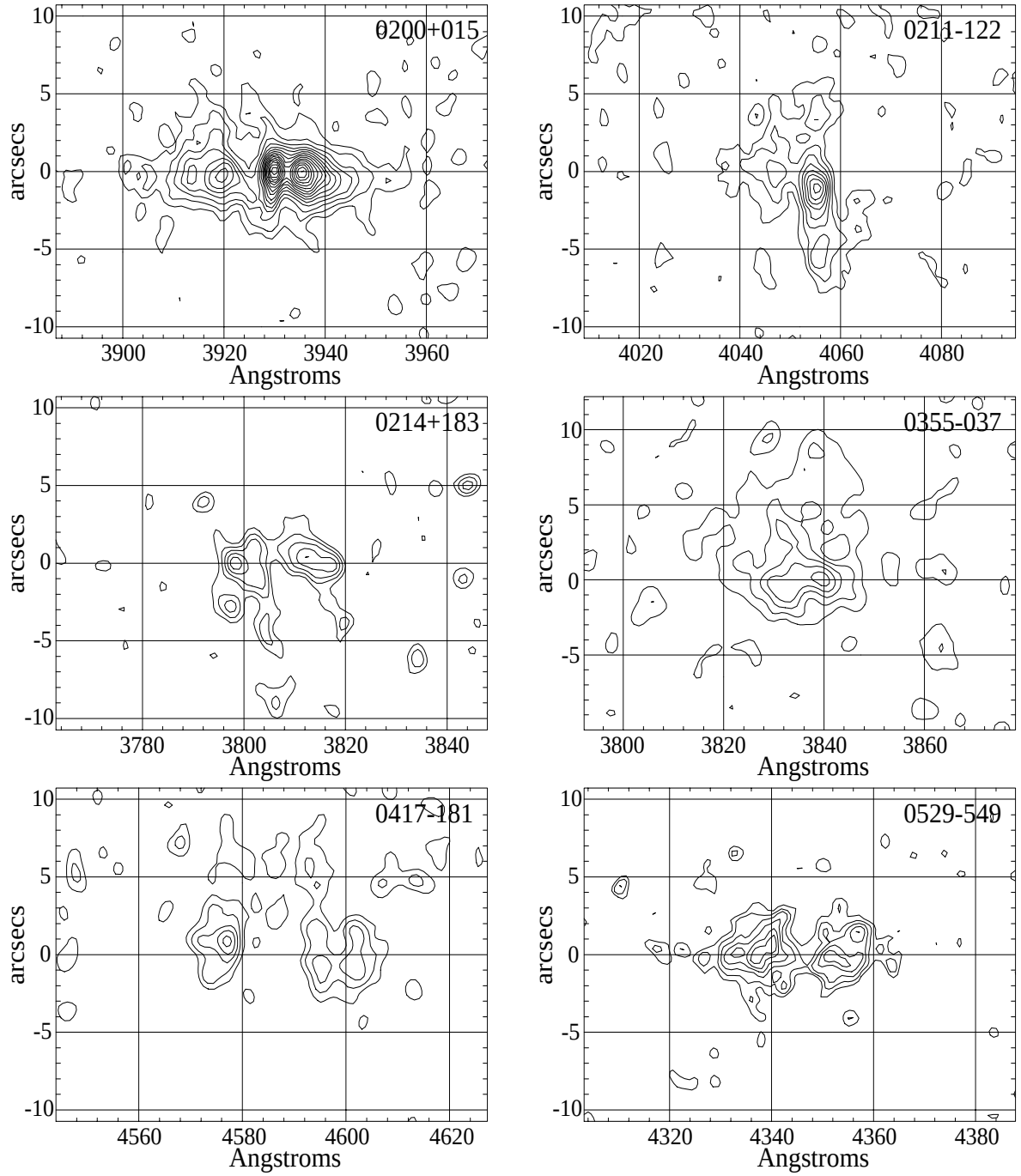

Fig. 1. Two-dimensional high resolution spectra of the Lyα emission regions. The two-dimensional spectra have been smoothed with Gaussian of $1'' \times 2$ Å (FWHM) to enhance the extended Lyα emission. The final resolution in these representations of the two-dimensional spectra is $\sim 1.2'' \times 3.5$ Å, except for those objects observed in $> 1''$ seeing (see Table 1 and 2). Because of the narrowness of the absorption features, the smoothing also results in the absorption troughs appearing less deep than in the unsmoothed one-dimensional spectra. In the spectra with the strongest Lyα lines, contours are linearly spaced at 2σ, 4σ, 6σ, etc., where σ is the RMS background noise. For the objects with fainter Lyα emission, 0214+183, 0417−181, 0529−549, 0748+134, 1357+007 and 2202+128, contours are linearly spaced at 2σ, 3σ, 4σ, etc

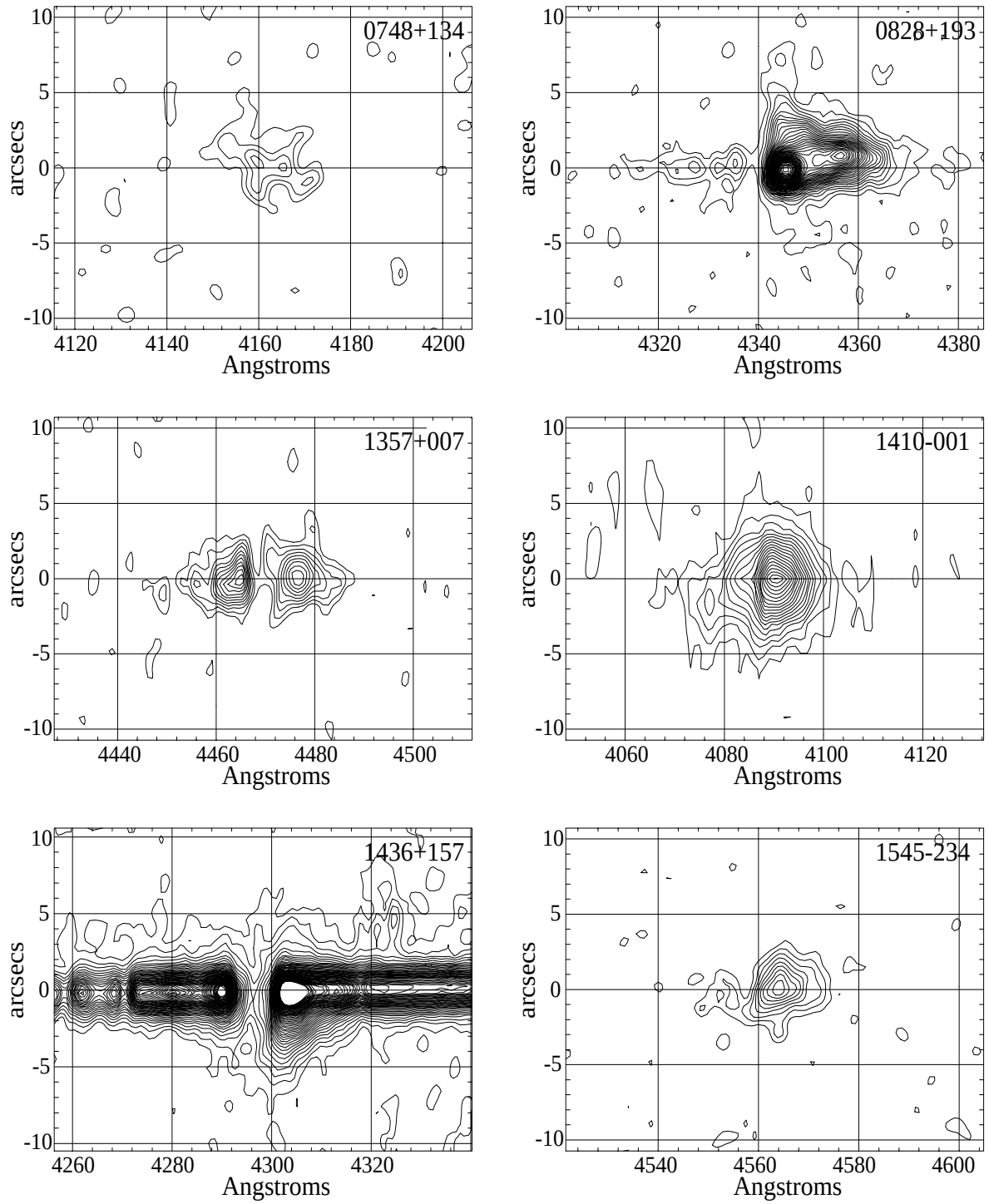

Fig. 1. – continued –.

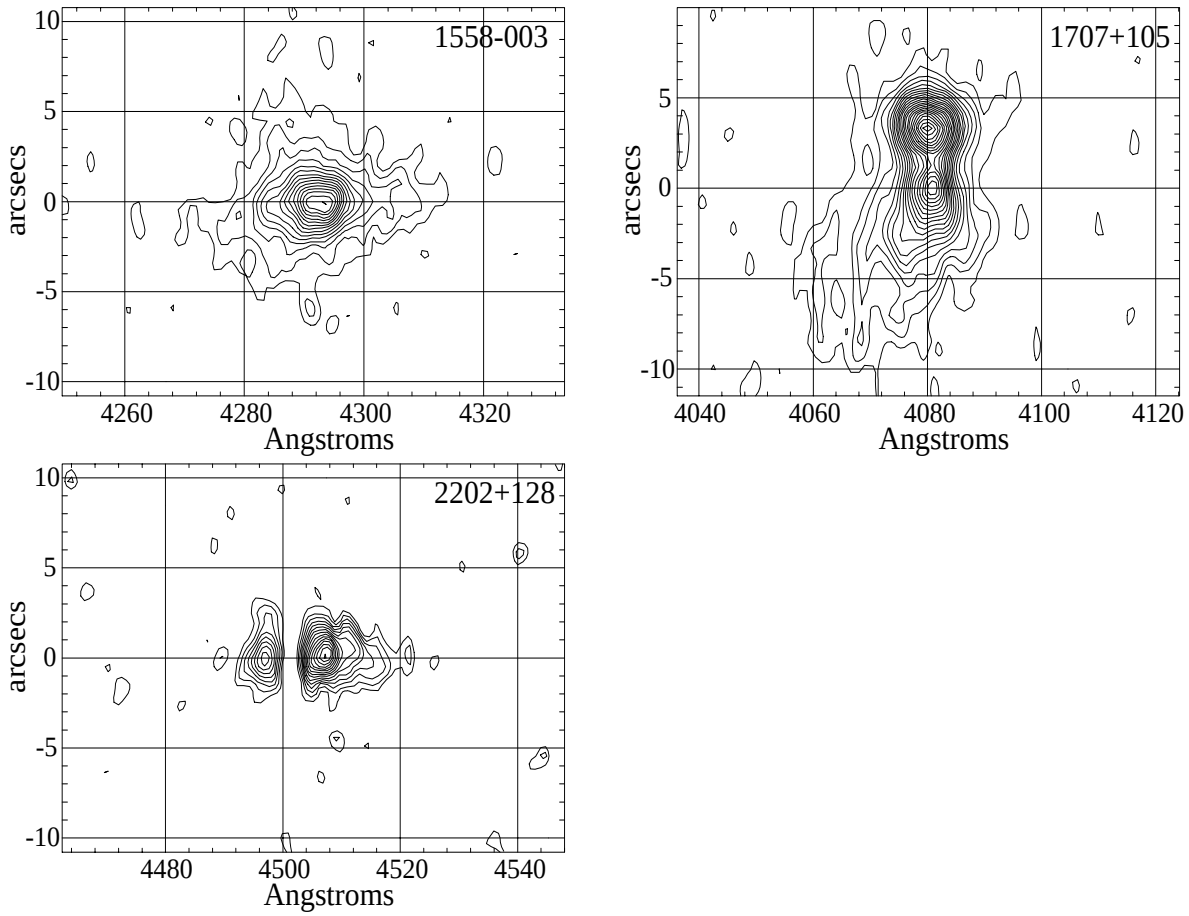

Fig. 1. – continued –.

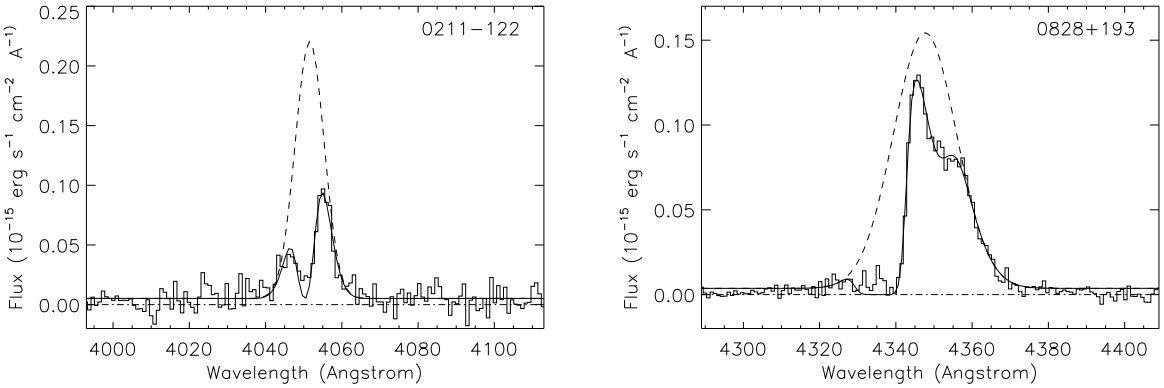

Fig. 2. *Left*: The profile of the "dusty" Lyα profile of 0211−122 fitted by an HI absorption with N(HI)=$10^{19.5}$ cm^{-2}. On the basis of our simple modelling assumptions, such strong HI absorption would be deeper than is observed. The solid line is the resultant profile from the model fitting, and the dashed line is the original Gaussian emission line profile calculated from the model fitting. *Right*: The absorption in the blue wing of Lyα in 0828+193 is modelled by one broad absorber. This model fits the steep drop from the Lyα peak well, but absorbs too much of the Lyα emission from the blue wing

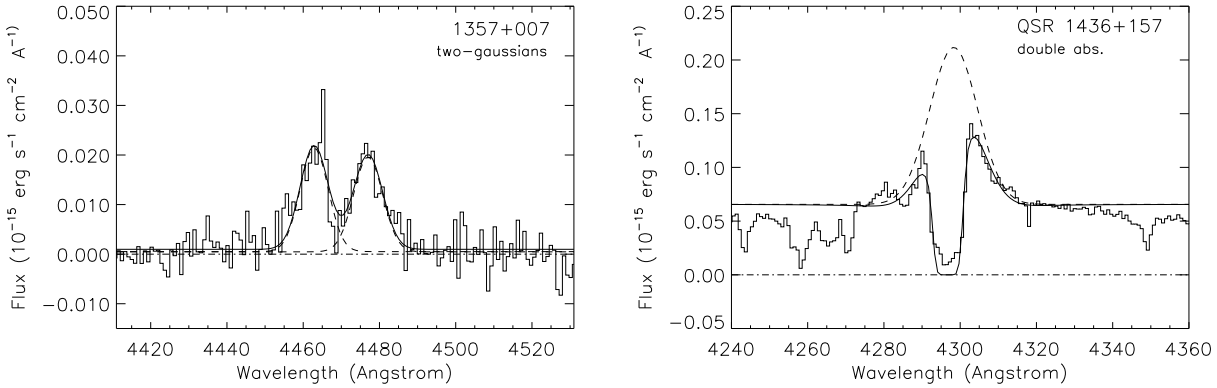

Fig. 3. *Left*: The double peaked Lyα profile of 1357+007 modelled by two separate Gaussian velocity components. The solid line is the resultant profile from the model fitting, and the dashed lines are the original Gaussian emission line profiles calculated from the model fitting. Note the inability of this model to closely fit the steep trough between the Lyα peaks, while the wings on either side are well fit by a Gaussian. *Right*: The strong absorption in the narrow Lyα component of the quasar 1436+157 modelled with two N(HI)$\sim 10^{19.3}$ cm^{-2} absorbers. A single absorber would require a very large Doppler parameter and gives a worse fit

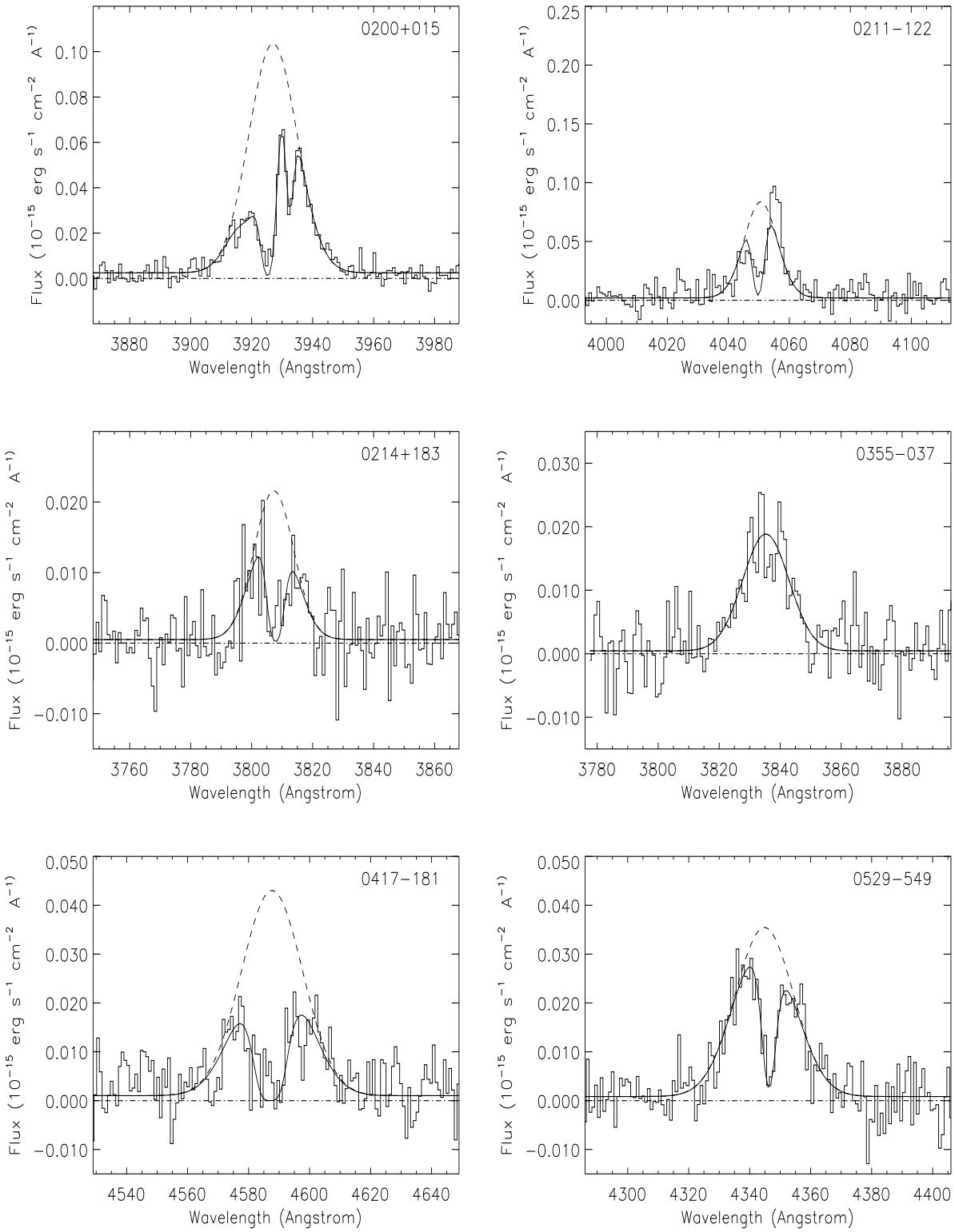

Fig. 4. Profiles of the Lyα emission lines. The solid line is the resultant profile from the absorption model fitting, and the dashed line is the original Gaussian emission line profile calculated from the model fitting

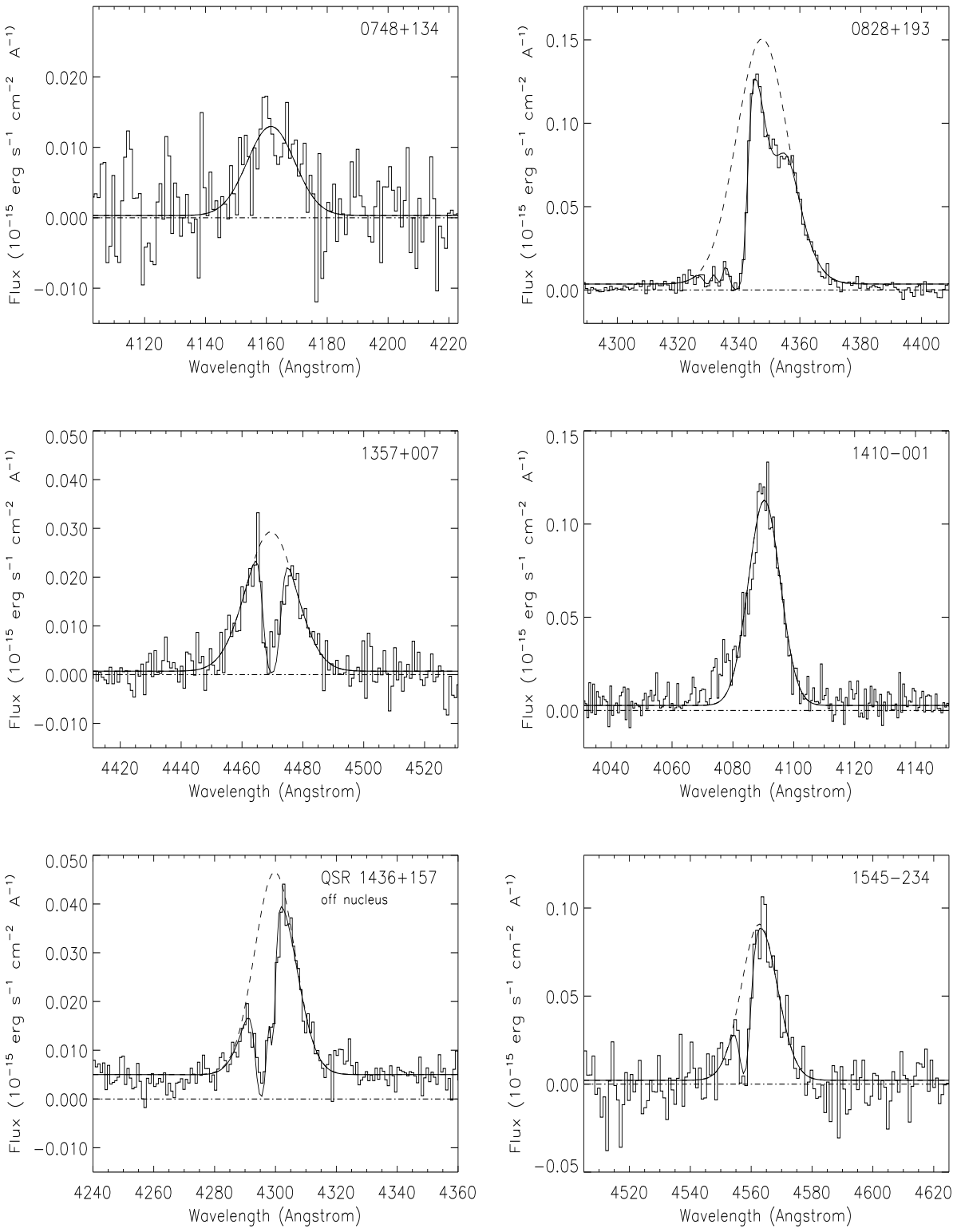

Fig. 4. – continued –.

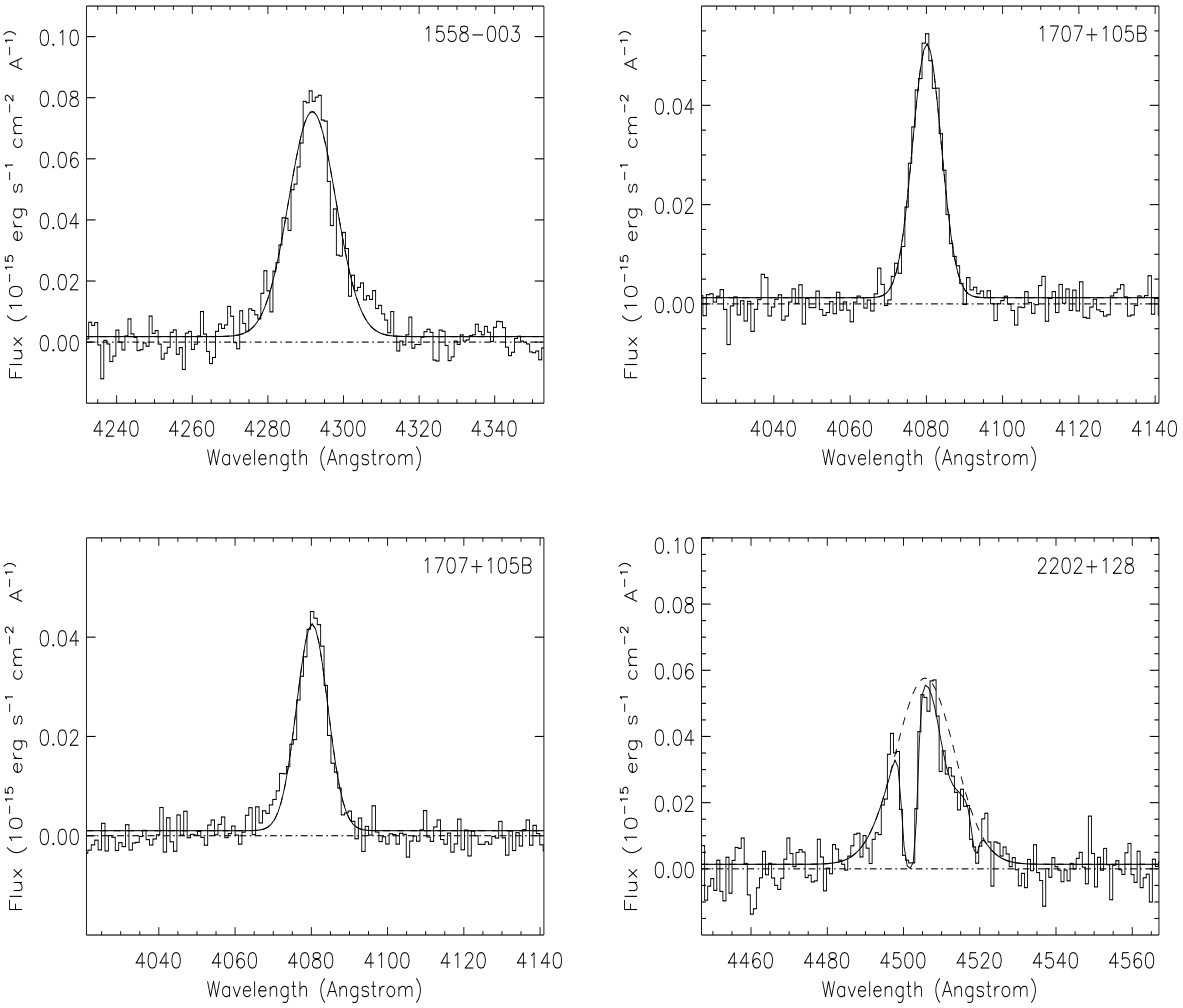

Fig. 4. – continued –.

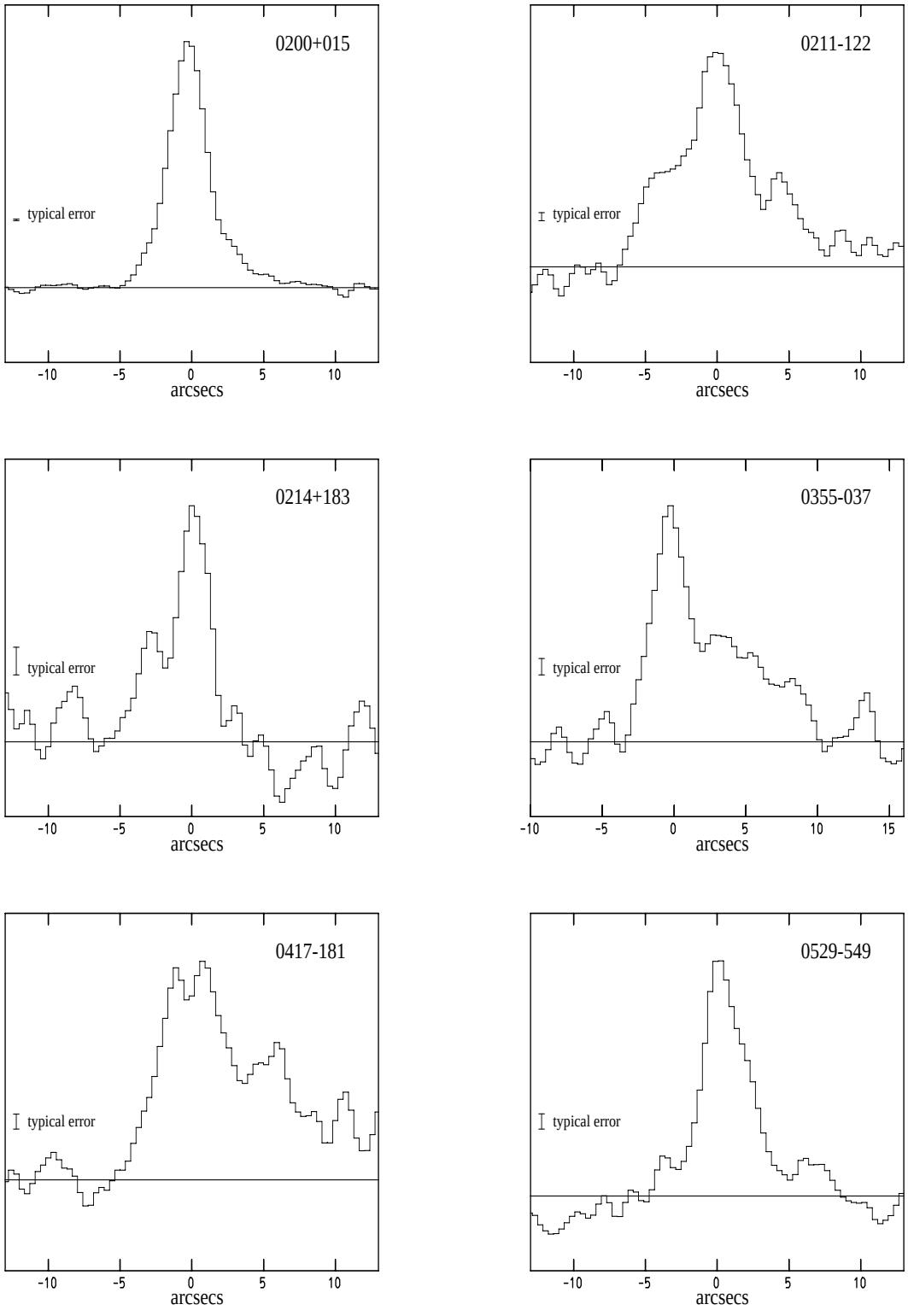

Fig. 5. Spatial profiles of the Lyα emission, summed over the full spectral range where Lyα emission was detected. The profiles have been smoothed with a Gaussian function of 1″ FWHM. The plots have an arbitrary y-axis scale. Also indicated is the 1σ error determined from the RMS background noise

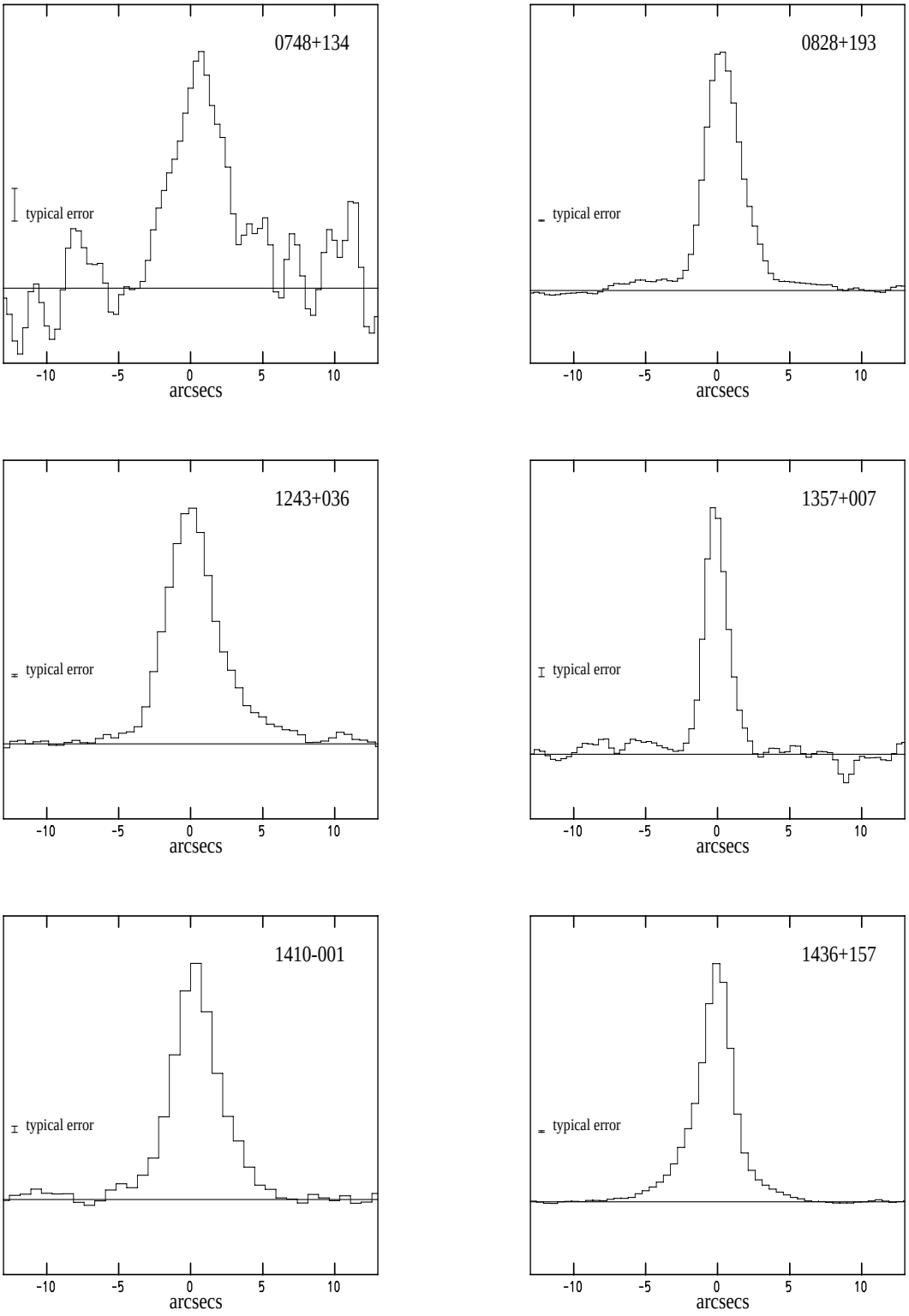

Fig. 5. – continued –.

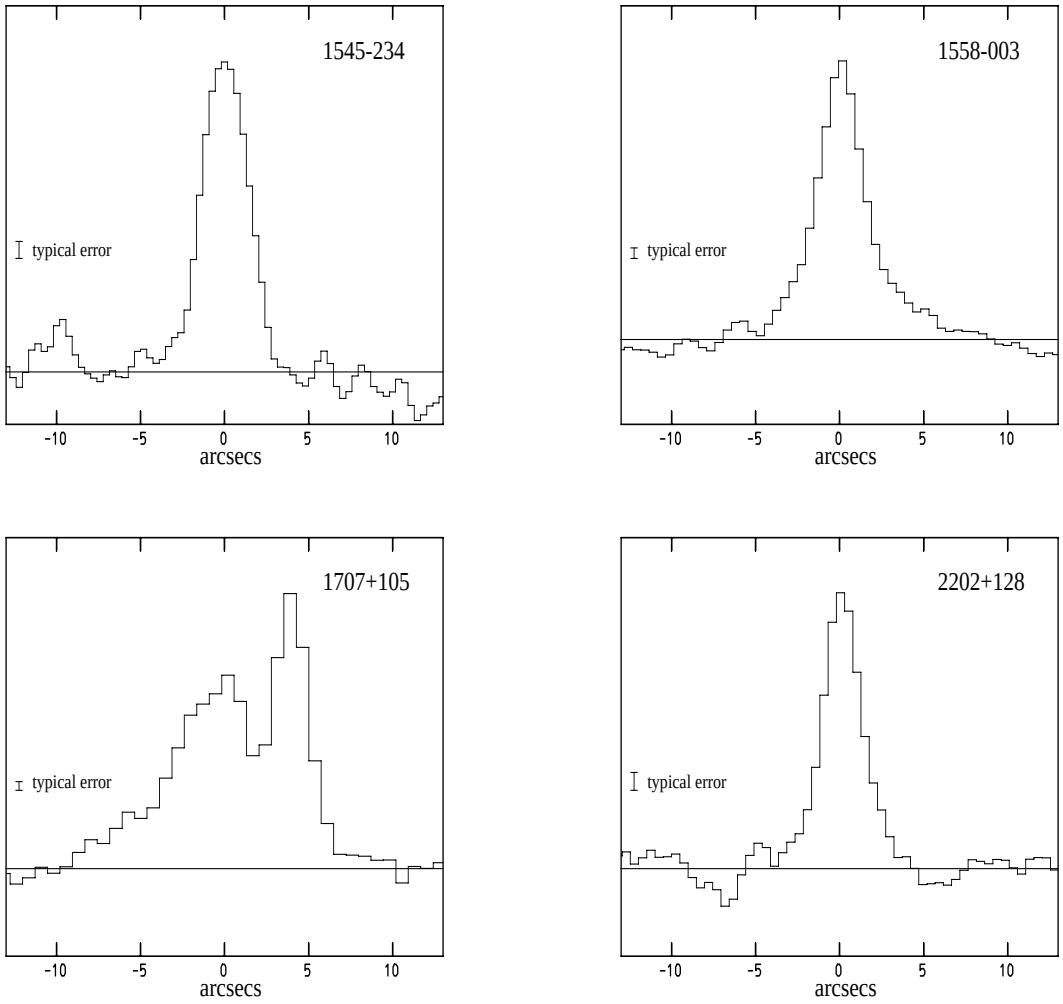

Fig. 5. – continued –.

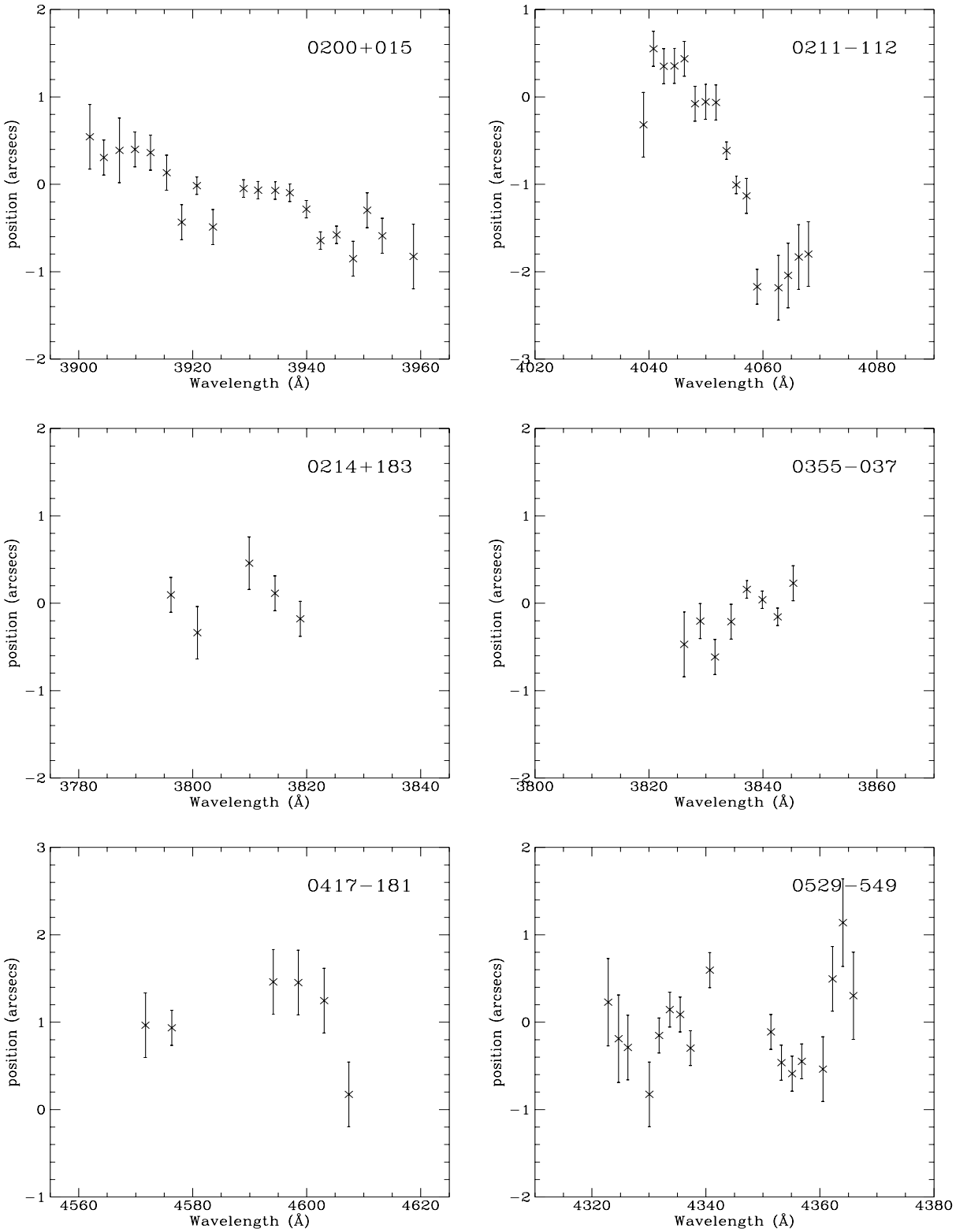

Fig. 6. Spatial positions of the maximum Lyα intensity plotted against wavelength

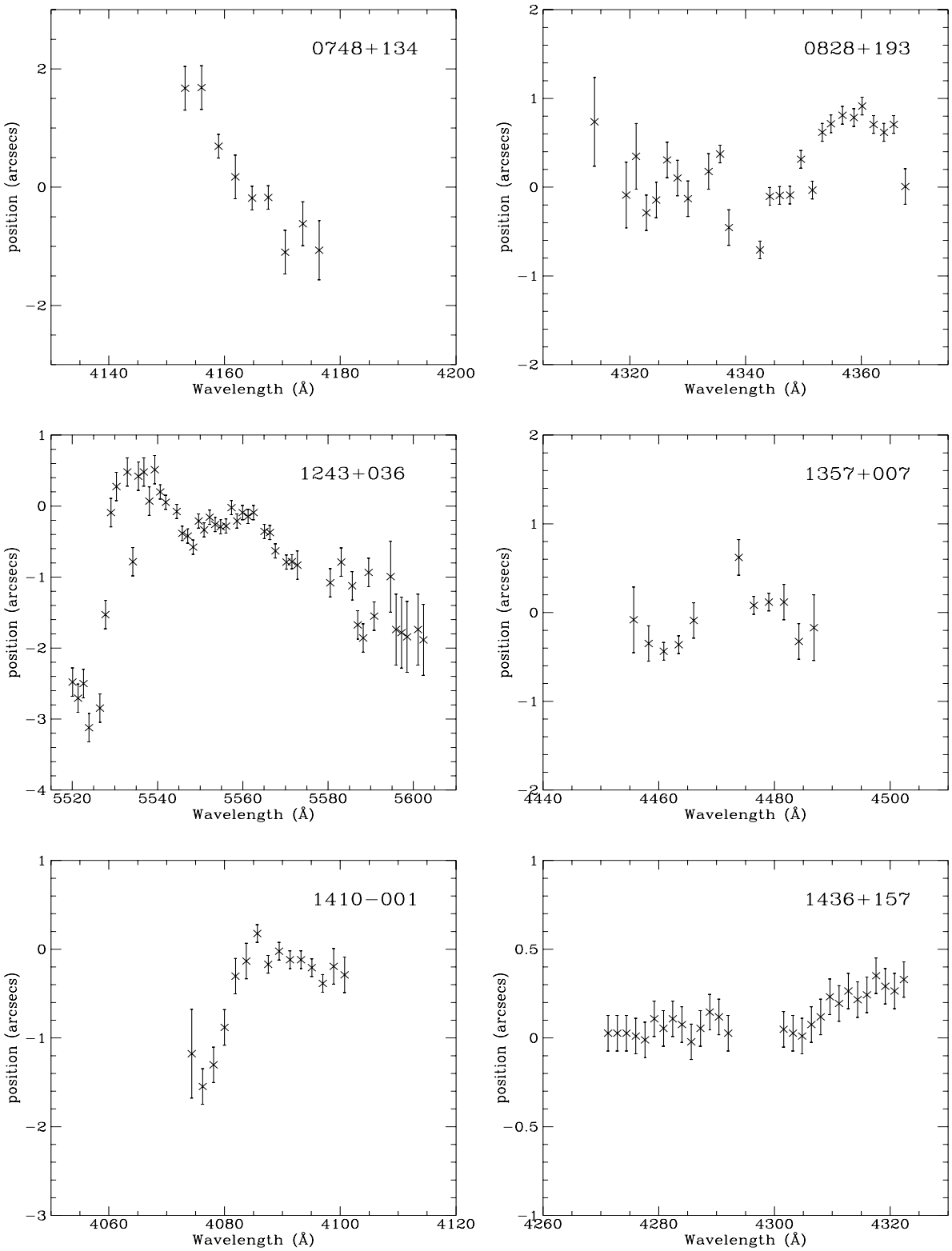

Fig. 5. – continued –.

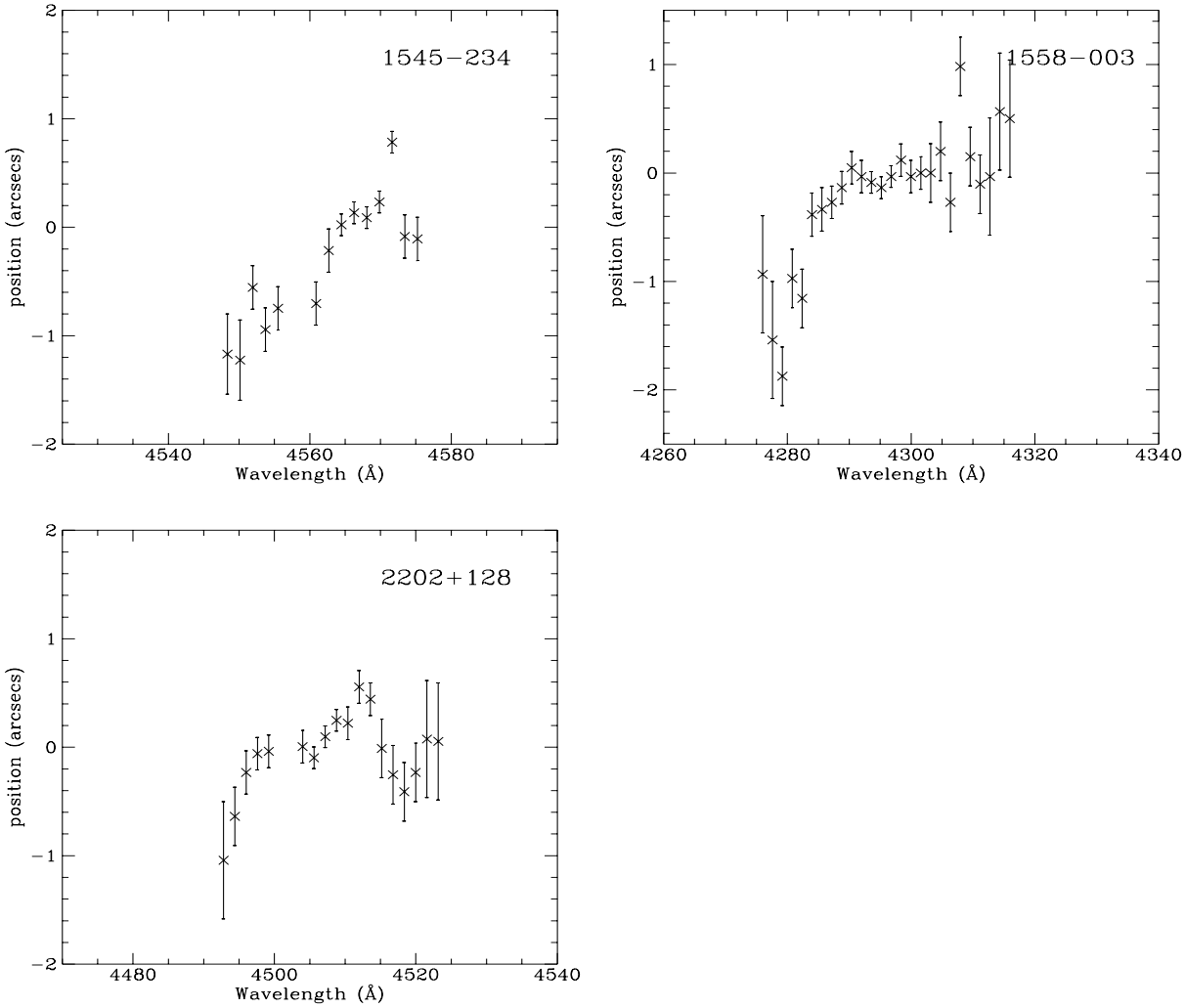

Fig. 5. – continued –.

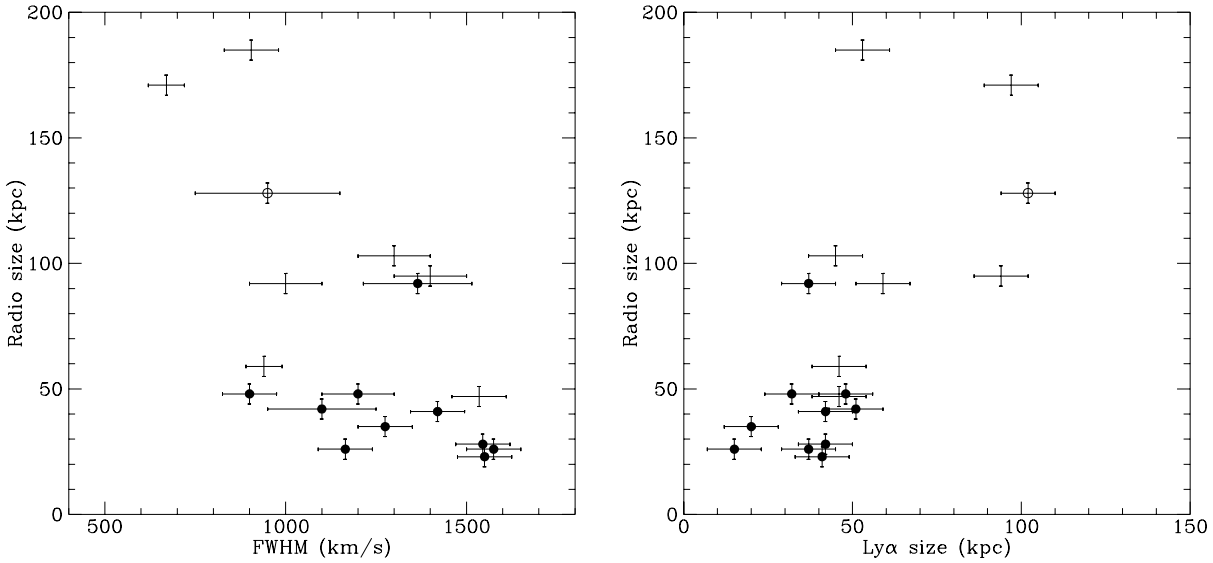

Fig. 7. **a** Radio size plotted against Lyα width (FWHM). **b** Radio size plotted against Lyα size, $D^{20\%}_{Ly\alpha}$. The objects marked with black dots are the ones with strong HI absorption (N(HI)$> 10^{18}$ cm^{-2}) in the Lyα profile. The object marked with an open circle is 0211−122 whose absorption is likely to be strongly influenced by dust (see text)

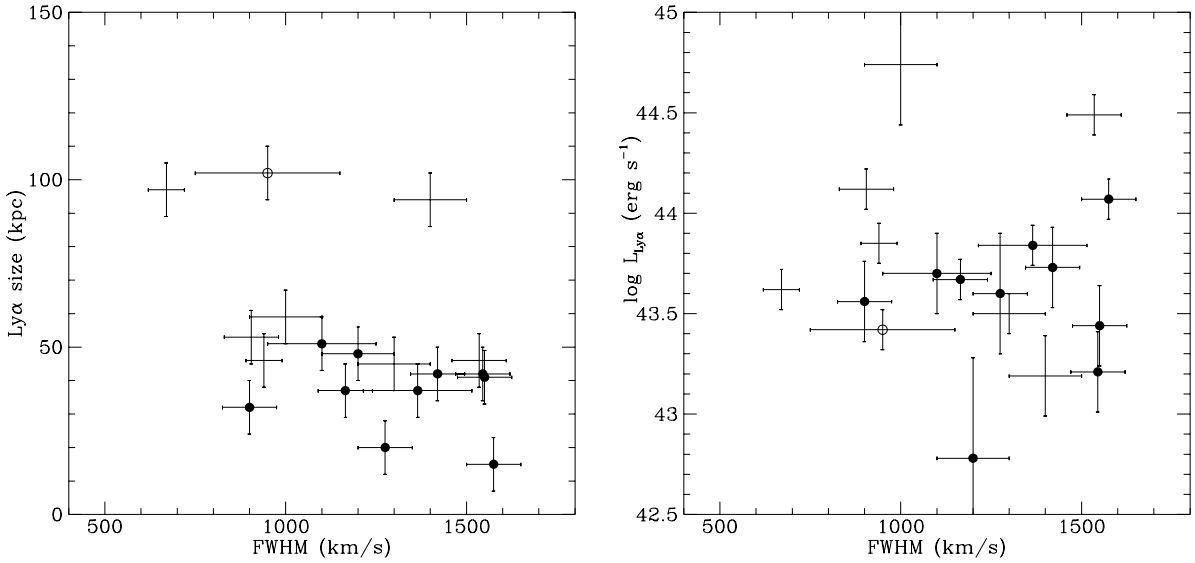

Fig. 8. **a** Lyα size, $D^{20\%}_{Ly\alpha}$, plotted against Lyα width (FWHM). **b** Lyα luminosity plotted against Lyα width (FWHM). The objects marked with black dots are the ones with strong HI absorption in the Lyα profile. The object marked with an open circle is 0211−122

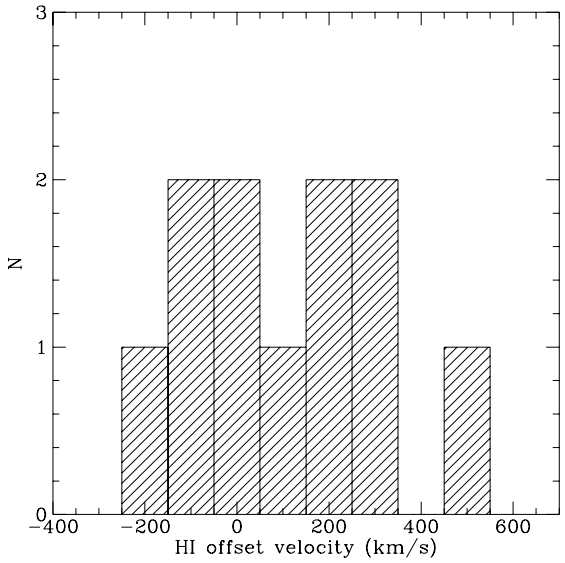

Fig. 9. Histogram of the relative velocities of the strong HI absorption systems (N(HI)> 10^{18} cm^{-2}) with respect to the peak of the Gaussian fitted to the Lyα emission. Negative velocities are redshifted with respect to the Lyα emission

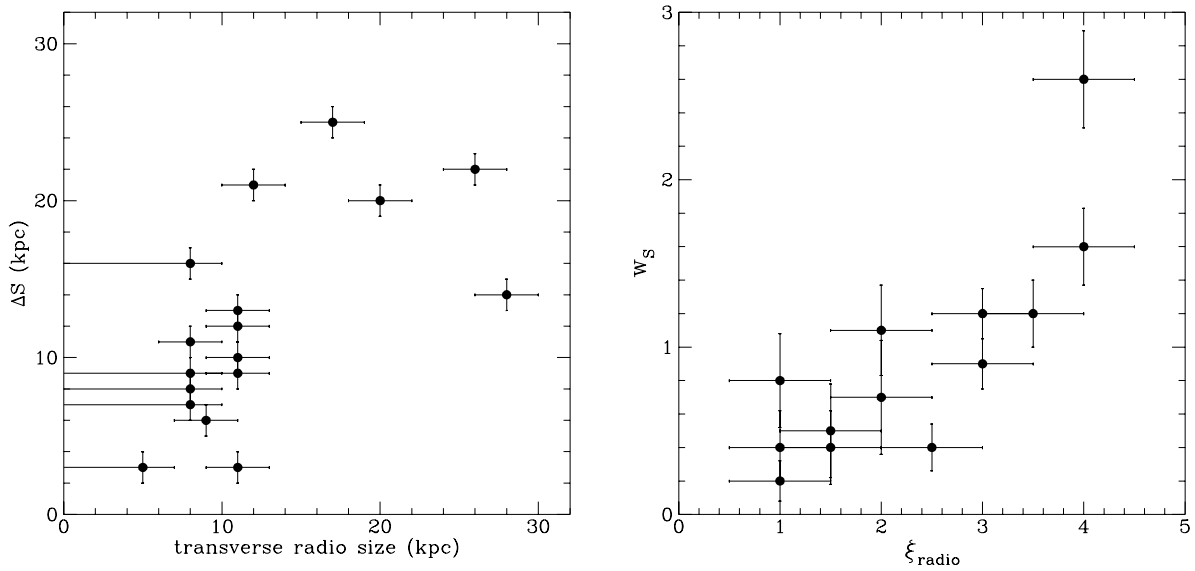

Fig. 10. a Maximum shift of Lyα peak position (ΔS) plotted against the transverse radio size. **b** "Wiggling index" of the Lyα position (w_S) plotted against the radio distortion index (ξ_{radio})

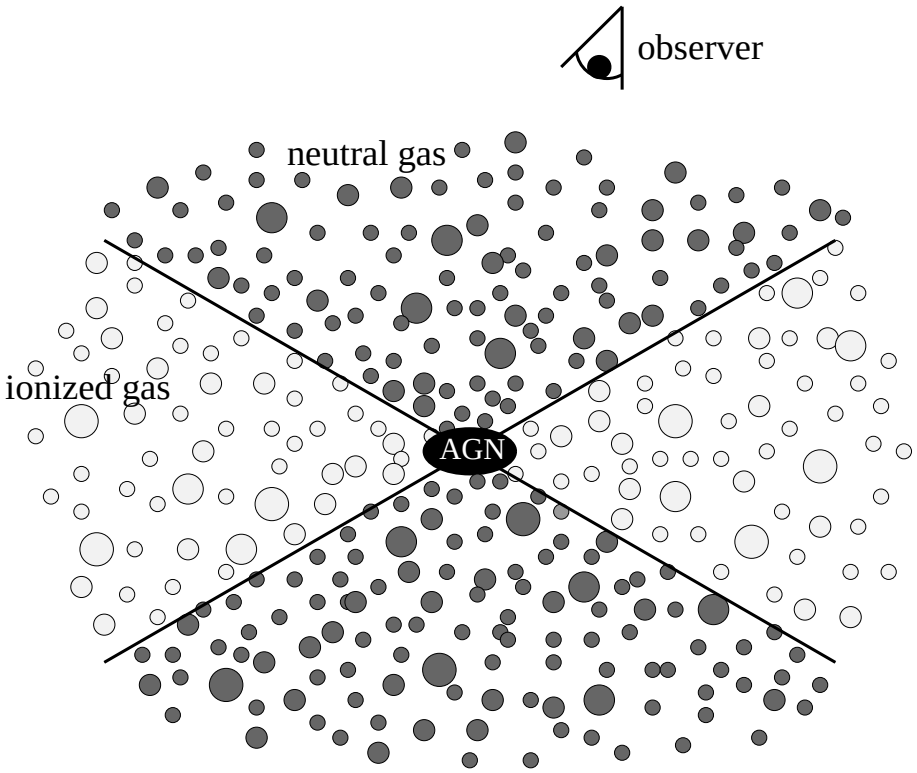

Fig. 11. Possible location of the absorbing gas in a radio galaxy with extended emission line gas according to an orientation-unification scenario. Gas in the ionization cone is photoionized by the AGN, while the gas outside the ionization cone is predominantly neutral and will cause absorption of Lyα emission when this is observed through the neutral gas. The velocity dispersion of the gas inside the ionization cone is increased by interaction with the radio jet. The gas outside the ionization cone is more quiescent and produces a narrow absorption feature in the Lyα emission profile

7 Tables

Table 1. High Resolution Spectroscopic Observations

Session	Date	Telescope/Instrument	Resolution	Average Seeing	Photometric
1	Nov 1992	ESO-NTT / EMMI	2.8 Å	1″	yes
2	Apr 1993	AAT	1.5 Å	2″	no
3	Nov 1993	ESO-NTT / EMMI	2.8 Å	1″	yes
4	Apr 1994	ESO-NTT EMMI	2.8 Å	1″	yes
5	Jun 1994	WHT / ISIS	1.7 Å	1.5″	no
6	Jan 1995	ESO-NTT / EMMI	2.8 Å	0.9″	yes
7	Apr 1995	ESO-NTT / EMMI	2.8 Å	1″	no

Table 2. Log of the observations

Source	z	Session	Total exposure time	Slit P.A.(°)
0200+015	2.230	6	7200 s	155
0211−122	2.336	3	5400 s	102
0214+183	2.131	1,6	7200 s	160
0355−037	2.151	6	8100 s	120
0417−181	2.770	3	10800 s	168
0529−549	2.572	1,3	10447 s	0
0748+134	2.410	6	5400 s	153
0828+193	2.572	4	5400 s	46
1357+007	2.671	4	7200 s	136
1410−001	2.359	2	8400 s	132
1436+157	2.550	5	6300 s	140
1545−234	2.754	7	9000 s	159
1558−003	2.520	5	7200 s	85
1707+105	2.345	4,5	18000 s	59,149
2202+128	2.704	5	5400 s	86

Table 3. Parameters of the H I absorbers

Source	$z_{Ly\alpha}$	z_1	log N(H I)$_1$ cm^{-2}	b_1 km s^{-1}	z_2	log N(H I)$_2$ cm^{-2}	b_2 km s^{-1}	z_3	log N(H I)$_3$ cm^{-2}	b_3 km s^{-1}	z_4	log N(H I)$_4$ cm^{-2}	b_4 km s^{-1}
0200+015	2.2312	2.2305	19.1 ± 0.2	56 ± 10	2.2364	15.7 ± 0.2	37 ± 10	2.2263	15.0 ± 0.5	480 ± 150			
0211−122*	2.3337	2.3335	18.5 ± 1.0	37 ± 20									
0214+183	2.1327	2.1341	19.5 ± 0.5	58 ± 10									
0355−037	2.1558												
0417−181	2.7749	2.7751	20.1 ± 0.4	26 ± 10									
0529−549	2.5750	2.5770	19.2 ± 0.3	10 ± 20									
0748+134	2.4242												
0828+193	2.5773	2.5709	18.1 ± 0.3	80 ± 40	2.5665	16.3 ± 0.3	55 ± 25	2.5632	16.2 ± 0.3	42 ± 20	2.5808	14.6 ± 0.5	300 ± 100
1357+007	2.6776	2.6786	18.5 ± 0.5	55 ± 15									
1410−001	2.3656												
1436+157	2.5379	2.5349	19.2 ± 0.4	12 ± 10	2.5379	15.4 ± 0.5	23 ± 20						
1545−234	2.7542	2.7507	18.2 ± 0.3	39 ± 10									
1558−003	2.5309												
1707+105A	2.3573												
1707+105B	2.3576												
2202+128	2.7082	2.7047	18.1 ± 0.2	48 ± 5	2.7189	14.8 ± 0.3	37 ± 10	2.7136	14.6 ± 0.3	350 ± 120			

*The two-dimensional Lyα profile of 0211−122 is probably affected by dust. The one-dimensional line profile is dominated by one narrow peak of emission but appears double peaked . This may be coincidental and the derived column density for possible HI absorption is very uncertain (see text).

NOTE– redhifts are calculated after conversion to vacuum values. Estimated formal errors on the redshifts are ~ 0.0002.

Table 4. Lyα parameters

source	FWHM$_{Ly\alpha}$ km s^{-1}	HIabs	D$^{20\%}_{Ly\alpha}$ kpc	D$^{tot}_{Ly\alpha}$ kpc	log L$_{Ly\alpha}$ erg s^{-1} cm^{-2}	M$_{Ly\alpha}$ 10^8 M$_\odot$	M(H I) 10^8 M$_\odot$	ΔS kpc	n_S	w_S
(1)	(2)	(3)	(4)	(5)	(6)	(7)	(8)	(9)	(10)	(11)
0200+015	1420±75	1	42	72	43.73±0.2#	2.0	3.1	11	1	0.2
0211−122	950±200	1	102	102	43.42±0.1	2.2	1.6	22	3–4	1.6
0214+183	1200±100	1	48	48	42.78±0.5#	0.8	2.6	6	1	0.5
0355−037	1400±100	0	94	105	43.19±0.2	1.6		7	1–2	1.0
0417−181	1550±75	1	42	42	43.21±0.2	1.1	4.9	10	1	0.4
0529−549	1550±75	1	41	45	43.44±0.2#	1.4	1.8	9	2	0.8
0748+134	1300±100	0	45	60	43.50±0.1	1.6		21	1	0.7
0828+193	1350±150	1	37	103	43.84±0.1	2.1	0.3	12	3	0.9
0943−242	1575±75	1	15	15	44.07±0.1	1.4	0.1	3	1	0.4
1243+036	1550±75	0	46	135	44.49±0.1	7		25	4	1.2
1357+007	1275±75	1	20	45	43.60±0.3	1.1	0.1	8	2	0.9
1410−001	900±75	0	53	79	44.12±0.1	3.5		14	2	1.1
1436+157*	1100±75	1	51	88	43.70±0.2#	2.1	6.0	3	1–2	0.4
1545−234	900±75	1	32	45	43.56±0.1	1.6	0.1	13	1–2	0.8
1558−003	950±50	0	46	77	43.85±0.1	2.4		16	1	0.4
1707+105	670±50	0	97	134	43.62±0.1	2.7				
2202+128	1150±75	1	37	37	43.67±0.1	1.7	0.1	9	4–5	2.6
4C41.17	1000±100	0	59	98	44.74±0.3	6.5		20	3	1.2

measured only from high resolution spectra, which sometimes underestimates the flux.
* 1436+157 USS quasar; the parameters are for the narrow line component only.
NOTE–The size parameter D$^{20\%}_{Ly\alpha}$ was defined because in the weakest Lyα regions, the most extended detected emission was at ∼20% of the Lyα peak flux. For those weakest sources D$^{20\%}_{Ly\alpha}$ is therefore equal to D$^{tot}_{Ly\alpha}$.

Table 5. Radio parameters

source	D_{Radio} (kpc)	D^{trans}_{Radio} (kpc)	ξ_{radio}	SI	CF %	Q	R	$\log P_{1.5GHz}$ (W Hz^{-1})
(1)	(2)	(3)	(4)	(5)	(6)	(7)	(8)	(9)
0200+015	41	8	1	−1.17	< 0.5	1.1**	1.3	27.87
0211−122	128	26	4	−1.27	3.8	1.8	2.0	28.54
0214+183	48	9	1–2	−1.05	1.4	1.4	1.7	27.92
0355−037	95	< 8		−1.43			1.8+	28.46
0417−181	28	11	1–2	−1.26	0.6	1.7	2.5	28.32
0529−549	23	< 8		−1.15				28.54
0748+134	103	12	2	−1.46		1.9**	1.0	28.50
0828+193	92	11	3	−1.23	21	1.3	1.0	27.65
0943−242	26	< 5	1	−1.20	< 0.5	1.0**	2.8	28.30
1243+036	47	17	3	−1.31	1.0	1.3	2.0	28.68
1357+007	35	< 8		−1.21				28.19
1410−001	185	28	2	−1.19	6.7	1.0	2.7	27.93
1436+157	42	11	2–3	−1.18	2.1	1.3	2.5	27.90
1545−234	48	11	1	−1.20	11	1.7	1.7	28.19
1558−003	59	< 8		−1.17		2.8*	2.2+	28.27
1707+105	171	< 8		−1.20		1.7*	8.8+	28.55
2202+128	26	11	4	−1.25	0.9	1.8	1.8	28.06
4C41.17	92	20	3–4	−1.33	0.6	1.5*	3.1	28.58

* measured from *R*-band-ID + 1.5GHz radio map.
** measured from *R*-band-ID on 4.7GHz radio map.
+ measued from 1.5 GHz radio map.
NOTE– 0355−037: no position accurate enough could be measured of *R*-band ID.
1357+007 and 0529-549: not well enough resolved on 20cm radio map and no high frequency radio map available.

Electronic Appendix

0200+015: This galaxy is associated with a small (5″) double radio source and is a typical example of luminous Lyα emission with strong H I absorption. Apart from one strong absorber (N(H I)$\sim 10^{18}$ cm^{-2}) it has two additional absorption systems of lower column density in the Lyα emission. On the two-dimensional spectrum we see that the main absorber does not cover the entire extent Lyα emission with the same absorbing strength, but shows some Lyα emission at the north-east extremity. This indicates that the column density or covering factor of the absorbing clouds changes over the extent of the Lyα emission.

0211−122: This radio galaxy has a peculiar optical spectrum in which the Lyα emission is anomalously weak compared to the higher ionization lines. This anomaly has been interpreted as being produced by dust mixed through the emission line gas which partly absorbs the Lyα emission (van Ojik et al. 1994). The two-dimensional high resolution spectrum of the Lyα shows a clearly different structure than the rest of the galaxies in our sample. There is one small region with strong Lyα emission that is relatively narrow (300 km s^{-1} FWHM) and is responsible for more than one third of the flux. Furthermore there are several weaker patches of Lyα emission distributed around the bright peak. The bright narrow peak is spatially offset by $\sim 1''$ from the peak of the continuum emission. This somewhat peculiar two-dimensional Lyα profile is consistent with the interpretation of van Ojik et al. (1994) that dust is mixed through the Lyα emitting gas of 0211−122. The bright narrow peak may be a region where the dust content is sufficiently low so that the Lyα photons can escape. In spite of the different appearance of the velocity field, the integrated line profile does show a double peaked shape. Although this double peaked appearance may be produced by dust within the Lyα region, it is also possible that an H I absorption system plays a role.

If we model the observed profile as being due to H I absorption of an originally Gaussian profile, we obtain a fit as displayed in Fig. 2 with a very narrow ($\sim$700 km s^{-1} FWHM) Lyα having a strong H I absorption of column density N(H I)=$10^{19.5}$ cm^{-2}. However, the centre of this absorption is not as opaque as it should be with such a strong absorption (see also the two-dimensional spectrum in Fig. 1). There is more Lyα emission from the bottom of the trough than in any of the other galaxies with strong HI absorption. Thus it seems unlikely that this simple model is correct. An alternative fit is given by a less luminous original emission profile, thus ignoring most of the emission from the bright narrow peak and giving an HI column density of $\sim 10^{18}$ cm^{-2} (displayed in Fig. 4). However, this fit is also not well matched to the observed profile. It may be that the profile is purely due to dust mixed with the ionized gas, extinguishing the resonant scattering Lyα photons, although we cannot exclude that H I absorptions contribute to the shape of the Lyα profile of 0211−122.

0214+183: The Lyα emission is double peaked over its entire spatial extent, although the spectrum does not have a high S/N due to the very blue wavelength of the redshifted Lyα.

0355−037: The Lyα profile is smooth and shows no signs of H I absorptions. Apart from the brightest Lyα emission, there is low surface brightness Lyα emission extending over about 10″ in the north-western direction, i.e. the direction of the brightest radio lobe.

0417−181: Although the spectrum has relatively low S/N, the Lyα emission has a deep and

wide trough over its entire spatial extent of ∼42 kpc. In the red part of the Lyα emission on the two-dimensional spectrum, there is a hint of another small absorption system. On the spectrum, the faint continuum of a galaxy at $\sim 5''$ north of 0417−181 is also visible.

0529−549: The $\sim$ 40 kpc extended Lyα emission has a clear deep trough in its profile.

0748+134: This object shows no signs of H I absorption, but there is a hint of a velocity shear in the Lyα emission. A more sensitive spectrum is required to confirm this.

0828+193: The Lyα profile has a spectacular shape. The emission is very strong but drops steeply on the blue side of the peak, while slightly further bluewards some Lyα emission is visible again. Thus, it appears that almost the entire blue wing of the Lyα emission profile has been absorbed. Also the most extended and fainter emission shows the same sudden drop at 4343 Å. This is a remarkable radio galaxy that has a close ($\sim 3''$) companion along its radio axis (Röttgering et al. 1995b). The presence of a close companion, from which no Lyα emission is detected, suggests that a neutral gaseous halo of this galaxy might be responsible for the absorption of the blue wing of the Lyα emission from 0828+193. However, it is not certain that the companion is at the same redshift, because no emission lines are detected. Also in the red wing of the Lyα profile, a broad shoulder is observed that may be due to multiple H I absorption systems or may be caused by intrinsic velocity structure of the Lyα emitting gas.

The steepness of the absorption trough next to the Lyα peak requires the absorber to have an H I column density of $\sim 10^{18.3}$ cm^{-2}. But the broadness of the absorption, extinguishing nearly all emission in the blue wing of Lyα, requires the Doppler parameter for a single absorber to be $\sim$ 162 km s^{-1}. This fit is displayed in Fig. 2. This absorption fit has removed too much of the original Lyα profile, as there is clearly emission observed just blueward of the sharp drop to zero at $\sim$ 4340 Å. Thus, the absorption may be due to the combination of several absorption systems at slightly different velocities with respect to the Lyα peak. The few small emission peaks that are left of the Lyα blue wing, are significant and can be well modelled by assuming three distinct absorbers (see Fig. 4). The main absorber has a column density of $\sim 10^{18.1}$ cm^{-2} and the other two are $\sim 10^{16.3}$ cm^{-2} with more reasonable Doppler parameters of 16 to 80 km s^{-1}. Although the absorption may be even more complex, this model is the simplest one that gives a satisfactory fit so we adopted these values. The broad shoulder in the red wing is also modelled by HI absorption with a large gas velocity dispersion, but we cannot exclude that it is caused by true velocity structure in the Lyα emitting gas.

1357+007: This galaxy which is associated with a small ($3''$) radio source has a deep trough in the Lyα profile. The Lyα profile has a relatively low S/N. The one-dimensional spectrum of this object is a good example for demonstrating the difference between modelling the troughs as being due to H I absorption and as being due to true velocity structure. The limitations of the models are illustrated by comparing the best fits obtained by a two velocity component emission model (Fig. 3) with those from an absorption model (Fig. 4). The fit of the Lyα emission profile by a combination of two Gaussian emission profiles at different velocities is less satisfactory than the H I absorption model. This is because the trough between the two peaks on the profile is steeper than the wings on the outside of the emission peaks. Although

we cannot exclude the possibility of a non-Gaussian but symmetric double peaked emission profile, this difference in steepness of the trough and the outer wings of the emission profile is accounted for by a Voigt absorption profile which is also the best fit for the troughs in the profiles with the best S/N. The actual situation may be more complicated than implied by the idealized assumptions of the models, but it seems that also in 1357+007 H I absorption is the more plausible interpretation in spite of the lower S/N ratio than in our best spectra.

1410−001: This galaxy has a large (185 kpc) associated radio source and very extended Lyα emission ($\sim$80 kpc) with no signs of strong H I absorption. However, it shows an obvious velocity shear in Lyα, that may well be due to rotation. The amplitude of the velocity shear is almost equal to the overall velocity width (FWHM) of the line.

1436+157: This is a quasar–galaxy pair oriented along the radio axis (like the galaxy-galaxy pair 0828+193). There is no direct evidence that the galaxy is at the same redshift as the quasar; only the quasar shows strong Lyα emission. Apart from very broad Lyα emission and strong continuum, as is common for quasars, the Lyα has a spatially extended narrow component. This is why we include it in our sample. A strong H I absorption feature is present in the narrow line component over the entire Lyα extent. The extended Lyα emission is larger than the radio source. Part of the emission may be due to the companion galaxy or a tidal interaction if the companion galaxy is indeed associated with the quasar.

The strong H I absorption feature in the narrow line Lyα component requires a very large Doppler parameter of $\sim$200 km s^{-1} when modelled by one single absorber. Although we cannot exclude the possibility of an absorber with such a large intrinsic velocity dispersion, a better fit to the data is obtained by a model of two or more absorbers. In Fig. 3 the fit is shown that we obtain for two adjacent absorbers, each with an H I column density of about $10^{19.3}$ cm^{-2} and Doppler parameters of 12–75 km s^{-1}. We have also extracted a spectrum of the off-nuclear Lyα emission by only summing the spectra beyond a distance of 2″ from the peak of the continuum (shown in Fig. 4). Although there is still some contamination from the quasar continuum in this spectrum, the contribution of broad Lyα emission is negligible. To fit the off-nuclear profile, either a single absorber with large Doppler parameter ($\sim$250 km s^{-2}) is needed or more than one absorber. As a most plausible fit we have adopted a two absorbers model, whose parameters are in Table 3.

1545−234: The Lyα profile of this radio galaxy has an absorption in the blue wing. The absorption does not cover the entire Lyα extent.

1558−003: This object shows no signs of H I absorption. The Lyα emission line appears to have a broad component, especially in the red wing. This galaxy also shows signs of a velocity shear in the Lyα kinematics.

1707+105: A galaxy with large associated radio sources and a companion galaxy along the radio axis. The Lyα emission is very extended ($\sim$130 kpc), where not only the radio galaxy itself (A) but also the companion galaxy (B) shows strong Lyα emission. On the opposite side of the radio galaxy is a region of faint Lyα emission with a relative blueshift that seems to increase with distance from the radio galaxy. The Lyα emitting gas has a relatively low velocity dispersion and shows no signs of H I absorption.

2202+128: The radio and Lyα size of this galaxy are small ($\sim$35 kpc) and the Lyα profile shows a strong H I absorption feature just bluewards of the peak and a somewhat weaker absorption feature in the red wing at 4518 Å. Further the profile shows a flattened "shoulder" in the red wing (see Fig. 4).

Taking the small peak next to the absorption at 4518 Å to be real and assuming that the "shoulder" is also due to absorption, implies a very broad absorption (Doppler parameter ~ 450 km s^{-1}). An alternative model ignoring the small peak next to the absorption at 4518 Å gives similar values for the two sharp absorptions as in the first model, but involves a much lower Doppler parameter (~ 230 km s^{-1} to account for the "shoulder". It is possible that the shoulder in the red wing of the emission profile is indeed caused by an H I absorption system with a large intrinsic velocity dispersion or by a superposition of many small absorbers over this velocity range. However the underlying Lyα emission profile may not be strictly Gaussian and the "shoulder" may be due to true velocity structure of the Lyα emitting gas.